



**HAL**  
open science

# Mid- to Late-Holocene coastal morphological evolution, vegetation history and land-use changes of the Porto Gulf UNESCO World Heritage site and its surroundings (NW Corsica Island, Western Mediterranean)

Matthieu Ghilardi, Jordi Revelles, Jean-Baptiste Mary, Federico Di Rita,  
Claire Delhon, Sébastien Robresco

## ► To cite this version:

Matthieu Ghilardi, Jordi Revelles, Jean-Baptiste Mary, Federico Di Rita, Claire Delhon, et al.. Mid- to Late-Holocene coastal morphological evolution, vegetation history and land-use changes of the Porto Gulf UNESCO World Heritage site and its surroundings (NW Corsica Island, Western Mediterranean). *The Holocene*, 2023, 33 (9), pp.1023-1044. 10.1177/09596836231176492 . hal-04116323

**HAL Id: hal-04116323**

**<https://hal.science/hal-04116323v1>**

Submitted on 5 Jun 2023

**HAL** is a multi-disciplinary open access archive for the deposit and dissemination of scientific research documents, whether they are published or not. The documents may come from teaching and research institutions in France or abroad, or from public or private research centers.

L'archive ouverte pluridisciplinaire **HAL**, est destinée au dépôt et à la diffusion de documents scientifiques de niveau recherche, publiés ou non, émanant des établissements d'enseignement et de recherche français ou étrangers, des laboratoires publics ou privés.

1  
2  
3 1 **Mid- to Late Holocene coastal morphological evolution, vegetation history and land-use changes of**  
4 2 **the Porto Gulf UNESCO World Heritage site and its surroundings (NW Corsica Island, Western**  
5 3 **Mediterranean)**  
6  
7  
8

9 5 **Matthieu Ghilardi<sup>1</sup>, Jordi Revelles<sup>2,3</sup>, Jean-Baptiste Mary<sup>4</sup>, Federico Di Rita<sup>5</sup>, Claire Delhon<sup>6</sup>, Doriane**  
10 6 **Delanghe<sup>1</sup>, Sébastien Robresco<sup>7</sup>**

11 7 **Abstract**

12 8 Two coastal areas located on the North-Western side of Corsica Island have been investigated to  
13 9 reconstruct their Mid- to Late Holocene landscape evolution together with the history of human  
14 10 occupation. Particular attention has been paid to the study of shoreline migration and vegetation  
15 11 history alongside land-use. Three boreholes were drilled to a maximum depth of 4.20 m and laboratory  
16 12 work comprised the identification of molluscs and pollen/NPPs as well as sedimentological analyses.  
17 13 Chronostratigraphy is based on a series of 18 radiocarbon datings and enabled to reconstruct the  
18 14 environments in the Fangu Estuary to the north of the World Heritage site over the last six millennia,  
19 15 and over the last four millennia on the Girolata coastal plain to the south. Palaeogeographic  
20 16 reconstructions of shoreline mobility are established for each site based on borehole  
21 17 chronostratigraphy analysis. In addition, two original pollen and NPPs diagrams were established for  
22 18 the Girolata and Fangu sites. These reveal that anthropogenic activities began to significantly impact  
23 19 local vegetation cover ca. 2500 years BP at Girolata, and ca. 2000 years BP at Fangu. Of particular  
24 20 interest, our work records the first complete pollen sequence in Corsica for Roman times at Girolata:  
25 21 first, the exploitation of cereals, grapevines and the development of husbandry is observed during the  
26 22 Roman Republic (500 BCE-0), followed by the almost exclusive cultivation of *Olea* sp. during the Roman  
27 23 Empire (0-500 CE). Following this, and using other regional pollen studies obtained for NW Corsica, we  
28 24 propose a regional evolution of the complex human-environment interactions for the last six millennia.  
29 25 Our results reveal a peak of regional forest decline (the most intense event recorded for the Late  
30 26 Holocene) from the 11<sup>th</sup> to the 16<sup>th</sup> centuries CE which can be attributed to the exploitation of wood  
31 27 resources during the Pisan and Genoese dominations of the island.  
32  
33  
34  
35  
36  
37  
38  
39

40 29 **Keywords : Palaeoenvironments, Vegetation history, land-use, UNESCO World heritage site, Coastal**  
41 30 **landscape, Corsica**  
42  
43  
44  
45

46 34 1. Introduction

47 35 The coastal wetlands of the Mediterranean are of particular interest when reconstructing short- to  
48 36 long-term human-environment interactions, mainly at a local scale, as is attested by the abundant  
49  
50

51  
52 <sup>1</sup>CEREGE – AMU-CNRS-IRD-Collège de France-INRAE, Europôle de l'Arbois BP 80 13545 Aix-en-Provence CEDEX 04, France.  
53 [matthieu.ghilardi@cnrs.fr](mailto:matthieu.ghilardi@cnrs.fr)

54 <sup>2</sup>Institut Català de Paleocologia Humana i Evolució Social (IPHES-CERCA), Zona Educacional 4, Campus Sescelades URV(Edifici  
55 W3), 43007 Tarragona, Spain.

56 <sup>3</sup>Universitat Rovira i Virgili, Departament d'Història i Història de l'Art, Avinguda de Catalunya 35, 43002 Tarragona,  
57 Spain

58 <sup>4</sup>University of Lyon 2, Hisoma, Collectivité de Corse

59 <sup>5</sup>University of Roma La Sapienza

60 <sup>6</sup>University of Nice – CEPAM CNRS

<sup>7</sup>SIGOSPHERE, Chazay d'Azergues, France

1  
2  
3  
4  
5  
6  
7  
8  
9  
10  
11  
12  
13  
14  
15  
16  
17  
18  
19  
20  
21  
22  
23  
24  
25  
26  
27  
28  
29  
30  
31  
32  
33  
34  
35  
36  
37  
38  
39  
40  
41  
42  
43  
44  
45  
46  
47  
48  
49  
50  
51  
52  
53  
54  
55  
56  
57  
58  
59  
60

literature treating this topic over the last decade (Di Rita and Magri, 2012; Fontana et al., 2017; Melis et al., 2017; Poher et al., 2017; Brisset et al., 2018; Pascucci et al., 2018; Marco-Barba et al., 2019; Revelles et al., 2019). The general calm conditions accompanying sediment vertical accretion allow the acquisition of continuous sedimentary series, making coastal wetlands suitable places to reconstruct Early- to Late Holocene environmental changes, using a series of sedimentological, geochemical and palaeoecological proxies (Sabatier et al., 2010; Marco-Barba et al., 2013; Brisset et al., 2018; Lopez-Belzunce et al., 2020; Giaime et al., 2022). Along Corsica's shoreline (~1050 km long) where human occupation is well attested and documented, two hundred brackish (mostly lagoons and swamps) to freshwater ponds are found (Ghilardi, 2020 and 2021). These latter could potentially be cored in order to improve our understanding of landscape configuration over the last six to eight millennia. Indeed, over the last decade, Corsica, the fourth largest Mediterranean island (area of ca. 8720 km<sup>2</sup>), has been studied in an attempt to reconstruct human-environment interplays with robust chronostratigraphies on the coastal zone (Currás et al., 2017; Ghilardi et al., 2017a; Revelles et al., 2019; Vella et al., 2019; Di Rita et al., 2022a). All these studies are based on pollen analyses and have focused on human-environment interactions since Neolithic times (Currás et al., 2017; Ghilardi et al., 2017a; Poher et al., 2017; Revelles et al., 2019; Vella et al., 2019; Di Rita et al., 2022a). Some of these studies have also revealed that most of the coastal plains formed during the Late Holocene due to a general mechanism of deltaic progradation of the river mouths (Currás et al., 2017; Ghilardi et al., 2017a) following a period of maximum sea incursion that can be dated slightly before the Mid-Holocene (Vacchi et al., 2016 and 2018; Revelles et al., 2019). The Porto Gulf UNESCO World Heritage site (listed in 1983) in NW Corsica covers an area of ca. 120 km<sup>2</sup> that includes the Girolata Gulf, the Scandola Peninsula and the Fangu River (Figure 1), where a small number of coastal wetlands can be identified on the coastal plains. Until now, no geoarchaeological studies have attempted to reconstruct the human-environment interplays during the Holocene for the entire UNESCO site. However, extensive archaeological surveys conducted since the mid- 2010s attest to the presence of humans over the last ca. 2500 years at least, corresponding to the Roman (Cibecchini and Dieulefet, 2014) and Medieval periods (Huser et al., 2017; Mary, 2021 and 2022). Nonetheless, there are few known remains that reveal the complete history of the human occupation and land-use practices during Protohistory, Antiquity, and the Middle Ages. Based on archaeological findings, the Girolata and Fangu coastal plains may possibly have served as natural harbours (protected bays) since Early Roman times when the seashore was probably located further inland. In order to elucidate these geoarchaeological questions and to locally reconstruct past morphological changes and vegetation dynamics as well as land-use, the two main coastal areas (Girolata Plain and Fangu Estuary) were investigated. The aim of the present paper is to provide additional pollen sequences in the NW area of Corsica in order to obtain a full view of the vegetation history at the regional scale and over the last millennia, as influenced by human activities and other factors determining landscape changes, in particular during Protohistory, Roman and medieval times.

## 2. Site presentation and archaeological settings

### 2.1. The Girolata Plain

#### 2.1.1. Topography and geology of the area

The Girolata Plain is situated south of the Scandola nature reserve (Figure 1) and covers an area of ca. 4 ha. Until recently, swamplands were present in the westernmost part of the plain which is drained by two intermittent streams: Girolata Stream (Fig. 2A) to the east and Novalla Stream (Fig. 2A) to the west. Both rivers drain primarily Upper Carboniferous/Lower Permian rhyodacitic rocks of volcanic origin in the upper part of the drainage basins, and monzogranite in the lowermost part of the river valleys (Vellutini et al., 1985 and 1996; Huser et al., 2017; Figure 2A). Locally, Palaeozoic micaschists

1  
2  
3 85 outcrops are identified to the west of the catchment (Figure 2A). The Girolata coastal plain is limited  
4 86 to the South East by a coastal barrier formed by well-rounded pebbles embedded within a matrix of  
5 87 gravels and coarse sands, turning the flat plain into a back-ridge depression (Figure 2B).  
6 88

#### 8 89 2.2.2. Previous geomorphological studies

9 90 In the late 2010s, geomorphological investigations (Huser et al., 2017) carried out in the north-eastern  
10 91 part of the Girolata Plain revealed a succession of different environments, starting from marine to  
11 92 shallow marine during the Middle Bronze Age (1800-1350 BCE), followed by mainly terrestrial  
12 93 environments, potentially dated after Antiquity. However, the rather low number of sedimentary  
13 94 sequences obtained and dated by only two radiocarbon datings were insufficient to enable a full  
14 95 reconstruction of the palaeogeography of the plain over the last four millennia. In addition, no  
15 96 information concerning past land-use and human-environment interactions was gained for this period.  
16 97

#### 18 98 2.2.3. Archaeological settings

19 99 There are no trace remains of human occupation for the Prehistoric and Protohistoric periods  
20 100 throughout the catchment areas of Novalla and Girolata Streams nor in the vicinity of the Girolata  
21 101 Plain. For the subsequent cultural periods, recent archaeological surveys have revealed an important  
22 102 phase of human occupation during Roman times, ranging from the late 3<sup>rd</sup> century BCE until the early  
23 103 7<sup>th</sup> century CE (Cibecchini and Dieulefet, 2014; Mary, 2014a; 2014b; 2014c; 2018; 2021 and 2022; Huser  
24 104 et al., 2017). The site of Chjesaccia, located on a smooth granitic outcrop and situated a short distance  
25 105 from the present day shoreline of the Girolata Plain (Figs. 2A and 2B) yielded important findings. This  
26 106 site is also situated a very short distance from the stratigraphic profile studied in 2017 (Huser et al.,  
27 107 2017). In particular, tegulae (flat roofing tiles) and different building structures (apses) have been  
28 108 discovered and can probably be associated to an important coastal site dating roughly from the 3<sup>rd</sup>  
29 109 century BCE to the 2<sup>nd</sup> to 3<sup>rd</sup> centuries CE (Mary, 2014a, 2014b, 2020). Recent archaeological  
30 110 excavations have revealed a building probably dated from the 1<sup>st</sup> century CE (Mary, 2020) located to  
31 111 the west of the plain, in the modern village of Girolata. Beyond the coastal plain and its immediate  
32 112 surroundings, the Novalla River valley evidences (surface surveys) the presence of material dated from  
33 113 the 2<sup>nd</sup> and 3<sup>rd</sup> centuries CE at two sites (Figure 2A) named Novalla (mid- main stream) and Calanchelle  
34 114 (upper stream; Mary, 2014a, 2014b).

35 115 Traces of modern nautical activity have been dated to the 16<sup>th</sup>-18<sup>th</sup> centuries CE (Cibecchini and  
36 116 Dieulefet, 2014) and remarkable buildings located primarily in the westernmost part of the Girolata  
37 117 Plain have been identified. The aim of these structures was both to protect the coastline from invaders  
38 118 (mainly the Ottomans, following the fall of Constantinople in 1453 CE) and to aid the development of  
39 119 agriculture. The configuration of Girolata Bay offers a protected coastline that may have served as a  
40 120 natural harbour. The construction of the nearby Girolata fort during the Genoese administration of the  
41 121 island is certainly related to the presence of such a harbour, as is revealed by recent submarine surveys  
42 122 (Cibecchini and Dieulefet, 2014).

43 123 The continuous occupation of the Girolata area over approximately two millennia (from the 3<sup>rd</sup> century  
44 124 BCE until the 18<sup>th</sup> century CE) confirms the important geostrategic position of the protected Bay on the  
45 125 western coast of the island and its role as a layover on the western Mediterranean maritime routes.  
46 126

## 48 127 49 128 50 129 2.2. The Fangu coastal plain

### 51 130 52 131 2.2.1. Present-day topography and geology of the surroundings

53  
54  
55  
56  
57  
58  
59  
60

1  
2  
3 32 The Fangu drainage basin covers an area of ca. 235 km<sup>2</sup> for a length of 24 km (Figure 1) and marks the  
4 133 northern limit of both the UNESCO world heritage site and the Corsican regional park. The catchment  
5 134 topography is characterised by steep slopes, with upper reaches situated at an elevation of 2335 m  
6 135 amsl (Capu Tafunatu; Figure 1) with the highest summit culminating at 2556 m (Punta Minuta; Figure  
7 136 1). The geology of the drainage basin can be divided into four main groups (Vellutini et al., 1985 and  
8 137 1996): 1/ the metamorphic and sedimentary complex which is located on the northern bank of the  
9 138 lower Fangu River valley. This complex dates from the Palaeozoic and is older than the volcanic  
10 139 complex of Monte Cintu (Vellutini et al., 1985 and 1996). The metamorphic complex includes pre-  
11 140 Devonian shales and schists (Figure 3A) while the sedimentary complex is made up of conglomerates  
12 141 and sandstones dating to the Devonian (Figure 3A); 2/ the volcanic complex of Monte Cintu dates from  
13 142 the onset of the Permian and composes half of the geology of the Fangu catchment. This complex  
14 143 consists of rhyolites of different colours (Figure 3A); 3/ To the east, rhyolites with ignimbritic facies  
15 144 form the eastern limit of the catchment where the higher summits are situated; 4/ The lower river  
16 145 valley is characterised by an abundant alluvial sedimentation due to multiple migrations of the Fangu  
17 146 River main course during the Quaternary. The river mouth does not connect with the sea at any time  
18 147 of the year but forms a large coastal swamp, situated in the former river estuary behind a thick and  
19 148 wide coastal barrier (Figure 3B), itself composed of rounded pebbles and a matrix of sands and gravels.  
20  
21  
22  
23  
24

#### 25 150 2.2.2. Archaeological settings

26 151 Human occupation of the area remains largely unknown due to the paucity of archaeological surveys  
27 152 conducted. However, the modern period is well represented with the identification of two towers built  
28 153 during the Genoese administration of the island. The first one was built in 1541 (Figs 3A and 3B) while  
29 154 the second was built in the same location in 1574. The construction of these towers supports the  
30 155 strategic position of the Fangu Estuary which, like Girolata Bay, probably served as a natural harbour  
31 156 on the road from Calvi to Girolata on the north-western coast of Corsica. Forest exploitation can be  
32 157 related to this coastal settlement, where wood trunks were transported from the uplands of the Fangu  
33 158 drainage basin to the estuary before being loaded onto boats. Sawmills located at Pozzona on the  
34 159 lower Fangu River were active between 1596 and 1608 CE (Graziani, 2004), and confirm this forest  
35 160 activity. Other than this, little is known in terms of human presence, in particular during Roman times.  
36 161 Many unanswered geoarchaeological questions remain concerning land use in the area, possibly linked  
37 162 to the Girolata sector.  
38  
39  
40

### 41 163 42 164 3. Methods

#### 43 165 44 166 3.1. Core sampling

45 167 Three 50-mm diameter vibracores were drilled reaching a maximum depth of 4.20 m (Figs. 2A, 2B, 3A  
46 168 and 3B). Each borehole was precisely mapped and subsequently levelled with topographic information  
47 169 derived from a LIDAR survey (Table 1).  
48  
49  
50

#### 51 170 52 171 3.2. Grain-size analyses

53 172 Samples were taken at 5 cm intervals. Many samples exhibited coarse particles (gravels to pebbles)  
54 173 above 2 mm. Wet-sieving by hand was then used to isolate the total fractions of coarse (>2 mm) and  
55 174 fine sediments (<2 mm). For the layers which contained fine particles only (less than 2 mm), laser  
56 175 diffraction grain-size analyses were undertaken. The grain-size distribution was measured using a  
57 176 Beckman Coulter LS 13 320 laser granulometer with a range of 0.04 to 2000 µm, in 116 fractions  
58 177 detected from 132 detectors (126 detectors for the scattering pattern and 6 detectors for the PIDS  
59  
60

1  
2  
3 78 (Polarization Intensity Differential Scattering) technology which is sensitive to sub-micron sized  
4 179 particles). The calculation model (software version 5.01) uses the Fraunhofer and Mie theory. For the  
5 180 calculation model we used water as the medium (RI = 1.33 at 20 °C) and a refractive index in the range  
6 181 of that of kaolinite for the solid phase (RI = 1.56; Buurman et al., 1996). Samples containing fine  
7 182 particles were diluted, enabling to measure between 8 and 12% of obscuration and between 45 and  
8 183 70% PIDS obscuration.  
9 184

### 12 185 3.3. Organic matter/carbonate content

13 186 Loss-on-ignition (LOI) measurements were conducted at CEREGE on cores Girolata 2 and Fangu  
14 187 following Dean (1974) and Bengtsson and Enell (1986). Sediment samples of approximately 10 to 20 g  
15 188 were taken at 5 cm intervals throughout the sequences. After drying at 105°C to constant weight, the  
16 189 samples were heated to 550°C for 7 h to estimate the organic content. A second heating phase to  
17 190 950°C for a further 7 h was undertaken to assess the proportion of carbonate.  
18 191

### 21 192 3.4. AMS dating

22 193 The chronostratigraphy of the cores was established using a series of 18 AMS radiocarbon  
23 194 determinations from charcoal, organic matter and plant remains (*Posidonia oceanica*) (Table 2). The  
24 195 analyses were conducted in the Poznan (Poland) Radiocarbon Dating Laboratory. <sup>14</sup>C ages were  
25 196 calibrated using Calib Software Version 8.2 (Stuiver and Reimer, 1993) and the IntCal20 calibration  
26 197 curve for terrestrial samples (Reimer et al., 2020). Marine samples (*Posidonia oceanica*) were corrected  
27 198 for the local marine reservoir effect according to Siani et al. (2000) and Reimer and McCormac (2002)  
28 199 where regional  $\Delta R$  is -109 ( $\pm 40$ ) in the area of Bastia (situated 75 km east of the study area). Finally,  
29 200 the age-depth models were built in Clam.r 2.2. (Blaauw, 2010) using best fitting methods, smoothing  
30 201 spline for Fangu and linear interpolation for Girolata 2 (Figure 4).  
31  
32  
33  
34  
35

### 36 203 3.5. Mollusc identification

37 204 Cores Girolata 1, Elbu and Fangu were devoid of molluscs, while Girolata 2 was rich in fossils. All  
38 205 samples were wet-sieved through a wire screen (0.40 mm mesh) and air dried at room temperature.  
39 206 The residue was examined under a binocular microscope (magnification:  $\times 10$ ) and all identifiable shells  
40 207 and characteristic fragments were selected and placed in separate plastic tubes. Based on the  
41 208 molluscan classification system which assigns Mediterranean species to well-defined ecological groups  
42 209 (Péres and Picard, 1964; Péres, 1982), bio-sedimentary units were then established for the present  
43 210 study.  
44 211

### 47 212 3.6. Pollen identification

48 213 Pollen analysis was focused on 20 samples from the shallow marine sequence of the Girolata 2 core  
49 214 and 24 from the Fangu core.

50 215 All (44) samples were processed following standard methods (Goeury and Beaulieu, 1979; Girard and  
51 216 Renault-Miskovsky, 1969) using treatment with HCL, NaOH, flotation in dense Thoulet liquor, HF and  
52 217 final mounting in glycerine. Around 300-350 pollen grains of terrestrial taxa were counted using an  
53 218 Olympus Bx43 microscope fitted with  $\times 10$  ocular lenses and  $\times 40/60$  objectives. Hygrophyte and aquatic  
54 219 plants (Cyperaceae, *Typha/Sparganium*, *Myriophyllum*, Ranunculaceae) and Amaranthaceae-  
55 220 Chenopodioidae were excluded from the pollen sum to avoid over-representation by local taxa. All  
56 221 pollen types are defined according to Reille (1992b). Cerealia-type was defined according to the  
57  
58  
59  
60

22 morphometric criteria of Faegri and Iversen (1989) (>40 µm pollen grain, >8 µm pore). *Alnus* spp. refers  
223 to some alder species, in particular *Alnus glutinosa* and *Alnus alnobetula* var. *suaveolens* (Req.) Regel.  
224 Non-pollen palynomorphs (NPP) identification followed van Geel (1978, 2001), van Geel et al. (2003),  
225 Revelles et al. (2016) and Revelles and Van Geel (2016). A percentage pollen diagram was created using  
226 Tilia software (Grimm, 1991-2011), and pollen zonation was defined using CONISS (Grimm, 1987); NPPs  
227 are described in the context of the pollen zones.

## 229 4. Results

### 230 4.1. General stratigraphy

#### 232 4.1.1. Girolata 1 core

233 This core is 3.15 m long and is characterized by the presence of very coarse material, mainly gravels  
234 and pebbles along most the sequence. However, four sedimentary units can be distinguished (Figure  
235 5):

236 - Sedimentary Unit 1 is found between 3.15 and 1.30 m deep and is characterized by an  
237 alternation between layers of grey sands containing balls of the Mediterranean seagrass *Posidonia*  
238 *oceanica* (depths of 2.95, 2.80, 1.92, 1.89, 1.82 and 1.66 m) and layers composed of gravels and a  
239 mixture of well-rounded and angular pebbles of dacites/rhyodacites. Unit 1 contains no molluscs, and  
240 with the exception of the layers containing *Posidonia oceanica*, the organic matter content is poor.  
241 Two radiocarbon datings were performed on fibers of *Posidonia oceanica* : in the lowermost part of  
242 Unit 1, at a depth of 2.96 m, an age of 1424-1047 cal. BCE was obtained, while in the uppermost part  
243 of the unit, at a depth of 1.66 m, an age of 1317-917 cal. BCE was recorded. Unit 1 is characteristic of  
244 marine environments with high energy of deposition, possibly in the supra tidal zone since no molluscs  
245 or shell debris were found. It is noteworthy that the lithology of the detrital material composed of  
246 gravels and pebbles is exclusively composed of dacites, the dominant rock of the Girolata catchment  
247 (Fig. 2).

248 - Sedimentary Unit 2 is identified from 1.30 to 0.80 m and its deposition began roughly in the  
249 early 1<sup>st</sup> millennium BCE, based on the radiocarbon dating results obtained for the top of the  
250 underlying Unit 1. Sedimentological features clearly exhibit a generally calm environment of deposition  
251 (clays), such as a coastal wetland where frequent terrestrial inputs are observed. The texture is a  
252 mixture of coarse materials, mainly gravels and angular pebbles (dacites), deposited within a  
253 sandy/clayey matrix. The lack of marine fauna and organic remains such as fibers of *Posidonia*  
254 *oceanica* may reflect a full terrestrial sedimentation rather than a marine origin of deposition inside  
255 the wetland.

256 - Sedimentary Unit 3 is found from 0.80 to 0.38 m. It consists of black organic clays with  
257 abundant organic remains and sharp pebbles of dacyte within the clayey matrix, thus indicating local  
258 detrital input into a swampland.

259 - Sedimentary Unit 4 is found between 0.38 m and the present day surface topography. It is  
260 composed of light orange to brown silts indicative of the modern soil plough.

261 Any palaeoecological (pollen based vegetation reconstruction) interest in these sedimentary units  
262 appeared to be very limited and was therefore not studied.

#### 265 4.1.2. Girolata 2 core

1  
2  
3 267 This core is 4.20 m long and encompasses the last 4.2 kyr according to chronostratigraphy based on  
4 268 the radiocarbon dating results (Table 2). Five main biosedimentary units (Figure 6) can be defined from  
5 269 the bottom to the top, as follows:

6 270 - Unit I is found between 4.20 and 2.95 m in depth and contains both marine molluscs and an  
7 271 abundance of fibers of *Posidonia oceanica*. This sedimentary unit is composed of silty clays and fine  
8 272 sands with mean grain size generally ranging between 50 and 150  $\mu\text{m}$ . Organic matter content is  
9 273 around 10 to 20%. The mollusc identification reveals strong representation of two main species:  
10 274 *Bittium reticulatum* (a marine gastropod) and *Loripes lacteus* (a shallow marine bivalve that lives on a  
11 275 sandy substratum), as well as *Cerastoderma glaucum*, *Clelandella miliaris*, *Tricolia pullus* and *Rissoa*  
12 276 *ventricosa* (not exceeding 5% in total). The mollusc assemblage clearly indicates the presence of a  
13 277 marine- to shallow marine environment dominated by a sandy sea bottom with development of the  
14 278 typical seagrass *P. oceanica*. It is noteworthy that this unit contains well preserved and identifiable  
15 279 pollen grains (see section 5.2.1). Radiocarbon dating was performed on the lowermost part of Unit I  
16 280 and reveals an age of 1921-1696 cal. BCE at a depth of 4.1 m. Towards the top of the unit at a depth  
17 281 of 3 m below the surface, an age of 1447-1286 cal. BCE was obtained. The above-described  
18 282 palaeoenvironmental proxies help to identify Unit I as a marine- to shallow marine environment  
19 283 (protected bay) with a sandy sea floor associated with calm dynamics of sedimentation. However, at  
20 284 the top of the unit, from 3.10 to 3 m deep, a thin layer of black organic sandy clays containing shell  
21 285 debris and some intact small specimens (juvenile) of *Bittium reticulatum* together with rare and intact  
22 286 *Cerastoderma glaucum* bivalves (of centimetric size) can be found. Also observed embedded within  
23 287 the clayey fraction were *P. oceanica* fibers. The top of Unit I (dated 1447-1286 cal. BCE) exhibits a clear  
24 288 transition to a more confined environment, still connected with the sea, and appears to correspond to  
25 289 a short phase of lagoonal development with very low energy of deposition.

26 290 - Unit II overlies Unit I and is found from 3 to 1.50 m below the surface. In general, it is composed  
27 291 of coarse material made up of sharp pebbles (dacites), angular gravels and medium to coarse sands.  
28 292 The radiocarbon dating performed at its transitions with Units I (below) and III (above) reveals that  
29 293 Unit II was deposited from ca. 1447-1286 cal. BCE to 650 cal. BCE, according to the estimation of the  
30 294 depth/age profile for this latter date. However, two sub-units can be distinguished and are described  
31 295 as follows: Unit IIA consists of grey medium to coarse sands with rare small fragments of marine  
32 296 molluscs (*Bittium reticulatum*) in its lowermost part. Several layers containing fibers of *Posidonia*  
33 297 *oceanica* are identified at the depths of 2.66, 2.55 and 2.20m: these fibers are abundant in the  
34 298 lowermost part of the unit. Unit IIB extends from 2.85 to 2.57 m and is composed of two layers of  
35 299 orange to red oxidized coarse sands (mean grain size ca. 400-600  $\mu\text{m}$ ) and sharp gravels, separated  
36 300 only by a thin layer (10 cm) of *Posidonia oceanica* and pebbles of dacite, dated to 1119-769 cal. BCE.  
37 301 No molluscs were identified in either of Unit IIB's oxidized layers, which may be indicative of terrestrial  
38 302 dynamics of deposition. In general, sedimentological results exhibit a higher energy of deposition in  
39 303 Unit II than in Unit I. The presence of rare debris of marine molluscs and balls of *P. oceanica* helps to  
40 304 characterize Unit II as part of a marine environment with high energy of deposition and where  
41 305 occasional terrestrial input can be observed at roughly the midpoint of the Final Bronze Age. Unit II  
42 306 can therefore be interpreted as a record of marine environments (intertidal to supratidal zone) with  
43 307 two isolated fluvial inputs (Unit IIB); it shows similar features and a date close to that of Unit 1 in  
44 308 Girolata 1 core.

45 309 - Unit III occurs between 1.50 and 0.40 m in depth. Age of deposition is well constrained and can  
46 310 be dated from ca. 650 cal. BCE to 1650 cal. CE, based on the dating of three samples of rich organic  
47 311 sediment (Table 2; Figure 6). It is composed of rich organic black clays (mean grain-size is around 5 to  
48 312 10  $\mu\text{m}$ ) with generally high organic matter content, comprised between 10 and 32% and decreasing  
49 313 towards the top of the unit. The highest values are recorded in the lowermost part of the unit with  
50 314 peaks situated above 25%. Unit III does not attest the presence of marine molluscs, but plant remains



1  
2  
3 15 and large pieces of wood are identified. Pollen content is high and well preserved grains were identified  
4 316 for reconstructing the past vegetation from the 7<sup>th</sup> century BCE to the 17<sup>th</sup> century CE (see section  
5 317 5.2.2.). Unit III shows similar sedimentological features to Unit 3 in Girolata 1 core.

6  
7 318 - Unit IV is found in the uppermost section of the core, from a depth of 0.40 m to the surface. It  
8 319 consists of modern soils with the presence of light orange to brown silts.

9 320

#### 10 321 4.1.3. Fangu core

11 322 The Fangu core is 4.20 m long and was drilled in the Fangu River estuary (Figs. 3A and 3B), which is  
12 323 disconnected from the sea during summer. Three main sedimentary units have been identified (Fig. 7)  
13 324 and no molluscs were identified along the sequence:

14 325 - Unit a is found from 4.20 and 3.50 m depth. It shows a transition from deeper layers of coarse  
15 326 material, mainly composed of very coarse sands and angular gravels, to higher homogeneous marine  
16 327 grey sands containing typical marine plant debris of *Posidonia oceanica* (top of the unit). A radiocarbon  
17 328 dating was performed at 4.12 m deep and gave an age of 3945-3653 cal. BCE (Table 2), while the  
18 329 uppermost part of the unit was dated to approximately 3 500 cal. BCE according to the depth/age  
19 330 modelling (Figure 7).

20 331 - Unit b is situated from 3.50 to 3.15 m depth. It consists of coarse material with low organic  
21 332 matter content (less than 5% on average), which increases towards the top. Sands and sharp gravels  
22 333 of rhyolite suggest a continental input since this rock forms half of the geological formations of the  
23 334 Fangu River. Age of deposition for Unit b is comprised between 3500 and 3100 cal. BCE (Figure 7).

24 335 - Unit c is located from a depth of 3.15 m to the surface and is relatively homogeneous (except  
25 336 for the sandy/gravelly layer identified between 1.15 and 0.85 m in depth), with organic clayey sand  
26 337 and peat layers. As a consequence, Unit c was studied for pollen identification (see below) which helps  
27 338 to characterize the environment of deposition. Radiocarbon dating performed in the lowermost part  
28 339 of Unit c (transition with Unit b) reveals an age of 3092-2907 cal. BCE (Table 2), which means that Unit  
29 340 c has been deposited over the last five millennia. Organic matter content shows the higher values (>  
30 341 10%) situated in the lowermost part of the unit: radiocarbon dating of these peaks reveals ages ranging  
31 342 from 3092-2907 to 2925-2692 cal. BCE. Between 1.15 and 0.85m, a layer of coarse material can be  
32 343 identified (Unit c1) which decreases gradually in terms of granulometry towards the top: the  
33 344 lowermost part of this layer (1.15-1 m) is composed of rounded gravels and small pebbles embedded  
34 345 within a clayey matrix, while the uppermost part (1-0.85 m) is characterized by coarse grey sands and  
35 346 intercalated beds of small gravels. The age of Unit c1 cannot be directly obtained with <sup>14</sup>C dating: the  
36 347 depth/age model provides an estimated age from the 4<sup>th</sup> century BCE to the 4<sup>th</sup> century CE., roughly  
37 348 corresponding to Roman times. In the upper part of the core (0.85 m deep to the surface), and  
38 349 corresponding to the return to the homogeneous grey clays of Unit c, numerous micro- and macro-  
39 350 charcoals are identified between 0.50 and 0.35 m, indicating a sustained fire activity: radiocarbon  
40 351 dating performed at 0.48 m deep reveals an age of 1179-1277 cal. CE, corresponding to the Pisan  
41 352 occupation of the island. It is likely that this rich charcoal content layer dates to the first half of the  
42 353 second millennium CE.

43 354

#### 44 355 4.2. Pollen results

45 356

##### 46 357 4.2.1. The Girolata pollen record

47 358 Two main pollen zones and two sub-zones were defined using CONISS (Grimm, 1987; Fig. 8):

48 359 - Sub-zone A1 (417-125 cm; 1845-406 cal. BCE) shows moderate values of AP (ca.50%), predominated  
49 360 by *Quercus ilex* and *Pinus*. In contrast, low values of *Quercus* deciduous, occurrences of *Fagus*, low  
50 361 values of *Alnus* and *Olea* are reported. High values of *Erica* (up to 40%), showing a decreasing trend,

high values of *Vitis* to the end of this sub-zone. A peak of Poaceae and occurrences of Cerealia-t at 1.40 m (625cal. BCE). Low values of Cyperaceae and Amaranthaceae (Fig. 8). Among the NPP, a high abundance of Foraminifera remains at 4.12-2.98m and an increase in monolete spores, *Spirogyra*, *Glomus*, *Coniochaeta* cf. *Lignitaria* and occurrences of coprophilous fungi (*Sporormiella*, *Sordaria*-t, *Cercophora*-t) at 125-140cm (Fig. 8).

- Sub-zone A2 (120-90 cm; 290 cal.BCE-482 cal. CE) reveals a decreasing trend in AP where *Quercus ilex* remains the predominant tree. At the same time, we observe a decrease in *Pinus*, an increase in *Quercus* deciduous (Fig. 8) and an increase in riparian trees, mainly *Alnus*; high values of *Olea* are also reported. Peaks of Poaceae and Cerealia-t are identified at the beginning and at the end of the sub-zone, with an increasing trend in Asteraceae, Apiaceae, Cyperaceae and Amaranthaceae at the end of the sub-zone. Among the NPP, we note high values in monolete spores, a continuous curve of *Spirogyra*, a decrease in *Glomus* and the lack of coprophilous and lignicolous/carbonicolous fungi (Fig. 8).

- Zone B (80-50cm; 839-1461 cal. CE): there is a sharp decrease in AP (ca. 20%), *Quercus ilex* and *Olea*, and very low values of *Quercus* deciduous and *Alnus*. At the same time, a decreasing trend in *Erica* is reported with an expansion of Cistaceae along with high values of Poaceae and occurrences of Cerealia-t. High values in Asteraceae, Apiaceae, Cyperaceae and Amaranthaceae (Fig. 8). Among the NPP, high values in monolete spores, a decrease in *Spirogyra*, an expansion of *Zygnema*-t, *Rivularia* and *Pseudoschizaea*, occurrences of lignicolous-carbonicolous fungi (*Coniochaeta*, *Kretzschmaria*, HdV-6, *Chaetomium*, UAB-4, 9, 11, 38) and coprophilous fungi (*Sordaria*-t, *Sporormiella*). (Fig. 8).

#### 4.2.2. The Fangu pollen record

Two main pollen zones and four sub-zones were defined using CONISS (Grimm, 1987; Fig. 9):

- Sub-zone A1 (200-190 cm; 2216-2082cal.BCE): high values of arboreal pollen (AP), predominated by *Pinus*, evergreen *Quercus* and riparian trees (*Alnus* spp., *Fraxinus*, *Salix*). This zone also shows low values of *Erica* and a remarkable peak of Cistaceae (Fig. 9).

- Sub-zone A2 (182-115 cm; 1962-507cal.BCE): we observe a slight regression in AP and *Pinus* and an expansion of *Erica*. High values of *Quercus ilex* and a slight decline in *Alnus* spp. are reported together with an increase in herb values (Poaceae, Asteraceae tubuliflorae, *Aster*-t) and a slight expansion in ferns (monolete spores, *Pteridium*, *Osmunda*-t and other trilete spores) (Fig. 9).

- Sub-zone B1 (83-66 cm; 316-740 cal. CE), a sharp decrease in *Pinus* values and later recovery (ca. 1500-1300 cal. BP) and opposite dynamics in *Erica*, expanding at *Pinus* regression.

- Sub-zone B2 (60-23 cm; 883-1632 cal. CE): minimum values of AP and *Pinus*, and a slight expansion of *Erica*. The expansion of NAP is predominated by Mediterranean shrubs (Cistaceae, *Helianthemum*-t, *Ephedra*, Lamiaceae) and grasses (Poaceae, Asteraceae, *Plantago*, *Artemisia*, Apiaceae). Occurrences of Cerealia-t at 28 and 34 cm (1435-1545 cal. CE). Occurrences of Amaranthaceae and Chenopodioidae and high values of Cyperaceae. Maximum values in monolete spores, *Polypodium*, *Isoetes*, *Pteridium* and *Osmunda*-t. Occurrences of *Pseudoschizaea* and type UAB-47 and maximum values of type HdV-36C.

401

402

403

404

405

## 5. Discussion

406

407

### 5.1. Palaeogeographic reconstruction of the coastal environments

408

09  
410 5.1.1. Shoreline reconstruction of the Girolata Gulf for the Late Holocene (Middle Bronze Age-Medieval  
411 Period/2200 cal. BCE-1800 cal. CE)

412  
413 *Mid- to Final Bronze Age (1800-800 BCE)* - Based on the sedimentological analyses and the mollusc and  
414 pollen identifications derived from Girolata cores 1 and 2, results indicate that the present day coastal  
415 plain remained under shallow marine conditions during the Middle Bronze Age (from ca. 1800 to  
416 1400/1350 cal. BCE; Fig. 10A). Indeed, a shallow and protected bay with a sandy-clayey bottom with  
417 *Posidonia oceanica* seagrass was present. Our results confirm the previous chronostratigraphic results  
418 obtained for the easternmost part of the area (Huser et al., 2017). During the whole period, for the  
419 westernmost part of the present day coastal plain, the shoreline position was located approximately  
420 150-175 m inland, while in the eastern part the coast was situated only 50 to 100 m further north, thus  
421 creating a deeper marine incursion to the west.

422 Following this, during the Late Bronze Age (1400-1250 cal. BCE), only the westernmost part of the study  
423 area was briefly occupied by a brackish lagoon (Fig. 10B), probably for less than a century in duration  
424 while landscape configuration in the easternmost part remains uncertain due to the paucity of  
425 chronostratigraphic data.

426 The Final Bronze Age (1200-800 cal. BCE) is characterised by generally higher energy of deposition than  
427 was previously observed during the Mid- to Late Bronze Age. The influence of the local streams on the  
428 coastal sedimentation is obvious and is confirmed by the presence of layers consisting of a mixture of  
429 angular pebbles and gravels of both monzogranite and dacites with *Posidonia oceanica* remains. Of  
430 note is the observation of a terrestrial input in the lower Novalla Stream valley only (Fig. 10C) at the  
431 onset of the Final Bronze Age. However, this detrital input is not homogeneous and two distinct phases  
432 of deposition composed of angular gravels of monzogranite embedded within an orange sandy matrix  
433 (rich in quartz) are observed, separated by a brief phase of marine sedimentation dating to the 1119-  
434 769 cal. BCE (median probability: 930 cal. BCE; Figure 6). The first phase of detritism, dated from ca.  
435 1250-1150 BCE, can be related to a local phase of erosion that affected the monzogranitic bedrock,  
436 situated primarily in the lowermost part of the Novalla catchment basin and in particular, on the  
437 western hills where the small village of Girolata is located today. Similar high continental input, dated  
438 to ca. 1200-1100 BCE, has been reported for the western coast of Corsica only, at the Canniccia pond  
439 situated in SW Corsica (Ghilardi et al., 2017b; Vella et al., 2019) and at Crovani for the period 1250-  
440 1150 BCE (Ghilardi, 2020; Di Rita et al., 2022a). Regional studies conducted around the Gulf of Lion in  
441 the western Mediterranean also evidenced a phase of strong alluviation centred around 1200-1000  
442 BCE, as is also the case in the Pyrenees (Galop et al., 2007) and in the lower Rhone River catchment  
443 (Berger et al., 2007). The existence of the so-called 3.2 kyr cal. BP Rapid Climate Change (RCC) event is  
444 suggested in the western Mediterranean with particular arid climate conditions (Mayewski et al., 2004;  
445 Magny, 2004; Magny et al., 2007; Fletcher et al., 2013). The origins of this brief period of heavy run off  
446 on the western coast of Corsica remain undetermined, but this area of the Mediterranean clearly  
447 experienced episodes of intense precipitations during a phase of prolonged aridity, in particular at the  
448 onset of the Final Bronze Age, ca. 1200-1100 cal. BCE.

449 Following a short return to marine conditions dated ca. 1000-900 BCE, at ca. 900-800 BCE, the Novalla  
450 stream underwent a second brief alluvial crisis, mainly affecting the granitic bedrock, as is revealed by  
451 the presence of an oxidized sandy layer. To the east, a large terrestrial input of the Girolata River is  
452 also attested, flowing into the shallow marine bay and triggering a mechanism of southward shoreline  
453 migration. Identification of this last phase of high continental detritism is based on the deposition of

1  
2  
3 54 sharp pebbles of rhyodacites and dacites that compose the upper reaches of the Girolata catchment.  
4 455 However, the exact dating of this detrital input remains unknown, even if its early phase of deposition  
5 456 can be dated approximately to the end of the Final Bronze Age/Early Iron Age, as suggested by the  
6 457 chronostratigraphy of the Girolata 1 core (Fig. 5). Following this and as a direct consequence, a lowland  
7 458 composed of coarse material deposited at the transition between the Final Bronze Age and the Early  
8 459 Iron Age formed, situated inland of a large coastal barrier system that primarily formed to the east and  
9 460 that advanced southwards. For the period 900-800 BCE, a mechanism of delta progradation based on  
10 461 a migrating coastal barrier system has also been reported for the same period for the Sagone River  
11 462 (Ghilardi et al., 2017a), situated approximately 30 km southwards. This morphological evolution of  
12 463 river mouths has been also observed along the coast of Tuscany for the Ombrone River (Pranzini, 2001;  
13 464 Bellotti et al., 2004; Biserni et van Geel, 2005) and in the Latium region for the Tiber River (Giraudi et  
14 465 al., 2009; Giraudi, 2011). Possible direct consequences of the 2.8 kyr cal. BP Bond event 2 (Iron  
15 466 Age/Homeric minimum; Bond et al., 1997), a period recognized for its sustained hydrological activity in  
16 467 the Western Mediterranean (Basetti et al., 2016), have been put forward to explain such deltaic  
17 468 advances. For the moment, there is no palaeoclimate reconstruction established for Corsica, so this  
18 469 question remains challenging, in particular along the western coast of the island.  
19  
20  
21  
22  
23  
24

25 471 *Iron Age, Roman and Medieval periods (800 BCE- 1800 CE)* - During the Iron Age and Roman times (Fig.  
26 472 10D), shoreline migration decelerated and enabled the formation of a large coastal barrier that  
27 473 extended along the entire paleo Bay of Girolata. To the west, a large coastal swampland developed  
28 474 with no significant detrital input from the Novalla Stream, from the Early Iron Age until modern times.  
29 475 The pollen record points to a freshwater environment, which was testified from 700 cal. BCE by high  
30 476 values of freshwater algae and riparian trees such as *Salix* and *Tamarix*. Then, a change towards a sub-  
31 477 aerial brackish marshland dominated by Cyperaceae and Amaranthaceae, with remarkable amounts  
32 478 of Apiaceae and ferns began around 550 cal. CE. This local environment persisted until the reclamation  
33 479 works of the plain in the 20<sup>th</sup> century CE (Fig. 10E). The regression of arboreal taxa and the high  
34 480 dominance of Asteraceae at 0.70-0.50 m at Girolata suggests soil formation (transition to a terrestrial  
35 481 environment) edaphisation for the last millennium according to the chronostratigraphy (Figure 6). In  
36 482 conclusion, the Roman period coincides with a more humid phase attested by the existence of a  
37 483 freshwater wetland, suggesting that wetter conditions and the availability of freshwater favoured the  
38 484 establishment of human populations in coastal areas of western Corsica during the Iron Age and the  
39 485 Roman period.  
40  
41  
42  
43  
44  
45

#### 46 487 *5.1.2. The Fangu Estuary: evolution over the last six millennia*

47 488 The sedimentary sequence collected in the Fangu Estuary reveals the presence of two main  
48 489 environments with contrasted energy of deposition. From ca. 4200 to 3500 cal. BCE, a marine  
49 490 environment prevailed in the western part of the present-day estuary (coring site). The presence of  
50 491 balls of *Posidonia oceanica* embedded within coarse sands and gravels indicates a high energy of  
51 492 deposition, probably related to an open marine bay. In the Mediterranean, the Mid-Holocene  
52 493 corresponds to a period of maximum sea incursion inland (Vacchi et al., 2016; 2018). Elsewhere in  
53 494 Corsica, this Mid-Holocene maximum marine incursion has been dated to 4000-3500 cal. BCE on the  
54 495 eastern coast, in the Aleria-Del Sale area (Currás et al., 2017) and on the North-West coast at Saint-  
55 496 Florent (Revelles et al., 2019). At both the Aleria and Saint Florent sites, the marine incursion was  
56 497 followed by a deceleration in sea-level rise that favoured the formation of coastal wetlands, mainly  
57  
58  
59  
60

1  
2  
3 98 lagoonal environments. Similar observations have also been reported in the Eastern Mediterranean  
4 499 with the onset of delta formations dated around 3500 cal. BCE (Brückner et al., 2005).

5 500 In the Fangu Estuary, the marine environment was followed by a phase of detrital input, probably  
6 501 linked to a deltaic advance of the Fangu River from ca. 3500 to 3100 cal. BCE. Isolation of brackish  
7 502 water behind a coastal spit favoured the formation of coastal wetlands shortly after that date.

8  
9 503 From ca. 3000 BCE until the present day, generally calm environments of deposition related to the  
10 504 formation of coastal wetlands have been recorded. However, a brief interruption in wetland  
11 505 deposition occurred from ca. 400 cal. BCE to 400 cal. CE marked by a fluvial input that persisted roughly  
12 506 throughout Roman times. The literature contains little evidence for such detrital input from Corsican  
13 507 rivers during Roman times, however an anthropogenic destabilization of the soils in the upper reaches  
14 508 of the Fangu River cannot be ruled out as a possible influence of this process. Climate conditions during  
15 509 the Roman period in the Mediterranean are recognised as being warm and wet, which possibly induced  
16 510 reinforced runoff in a context of diminished forest cover. As a result, the Fangu catchment may have  
17 511 experienced reinforced alluviation. Since the end of Roman times, landscape configuration has  
18 512 remained stable with the presence of coastal wetlands with salt intrusions. Our pollen record suggests  
19 513 that the Fangu lagoon may have been surrounded by riparian forests dominated by *Alnus*, *Fraxinus*,  
20 514 and *Salix* species, with prevailing freshwater conditions. Companion hygrophilous species of these  
21 515 riparian trees also seen to increase during this time interval are Cyperaceae and ferns (e.g. *Pteridium*,  
22 516 *Osmunda-t*, and other ferns with monoete spores (Figure 9). During the Middle Ages (750 cal. CE  
23 517 onwards), the development of Cyperaceae (Figure 9) reflects the expansion of shore environments  
24 518 leading to a regression of the lagoon and the expansion of sedges. Finally, the decline of sedge  
25 519 vegetation and the development of fern-dominated environments suggest drier conditions at local  
26 520 scale.

27 521 In general, prevailing freshwater conditions throughout the Late Holocene are also testified by the  
28 522 continuous record of freshwater algae, accompanied by low values of Amaranthaceae.

29 523  
30 524 5.2. Vegetation history of the UNESCO protected site (Fangu and Girolata coastal plains) and the  
31 525 influence of rapid climate changes during the Late Holocene

32  
33 526 The palynological study of cores Girolata 2 and Fangu enables the reconstruction of landscape for NW  
34 527 Corsica over the last 4200 years, from the Early Bronze Age to the Middle Ages. This helps to complete  
35 528 previous research conducted in the 1990s in the Fangu Estuary (Reille, 1992a) and in the 2020s in the  
36 529 Crovani pond (Di Rita et al., 2022a), respectively.

37 530  
38 531 *Bronze Age (4150-2750 cal. BP/2200-800 BCE)* - For the Porto Gulf UNESCO site, the vegetation has  
39 532 always been predominated by Mediterranean maquis, configuring an open landscape with *Erica* and  
40 533 Cistaceae, especially in Fangu, where *Erica* reaches 40-50% values (Figure 9). Pine and sclerophyllous  
41 534 forests played a secondary role in Girolata 2, while *Pinus* shows an important role in the area of Fangu,  
42 535 especially during the first half of the sequence (4200-2400 cal. BP/2250-450 cal. BCE). Mesic forests  
43 536 (*Quercus* deciduous, *Betula*, *Corylus*, *Tilia*, *Carpinus*) had a limited role in the landscape during the Late  
44 537 Holocene in this area, suggesting that climate conditions were more favourable to sclerophyllous  
45 538 vegetation in the lowlands. Of note is the limited presence of *Alnus* spp. riparian forests in this area  
46 539 compared with other Corsican areas, such as Saint Florent in the north (Revelles et al., 2019), Del Sale  
47 540 and Palo on the eastern coast (Currás et al., 2017; Revelles et al., 2019) and Sagone on the western  
48 541 coast (Ghilardi et al., 2017a). This may be due to the predominance of *Pinus pinaster* and *Pinus laricio*,  
49 542 accompanied by a maquis understory in granitic substrates at lower altitudes, as also occurs today in  
50 543 this area of Corsica. This would explain higher values in *Pinus* than *Quercus ilex* in Fangu, and the

1  
2  
3 44 limited presence of *Alnus* in both records. In this sense, during the period ca. 4200-2750 cal. BP (2250-  
4 545 800 cal. BCE/Bronze Age), pine forests played a significant role in the landscape in Fangu (Fig. 9),  
5 546 accompanied by *Erica*-dominated maquis.

6 547 Interestingly, from 4200 to 3900 cal. BP (2250-1950 cal. BCE) *Pinus* forest and *Erica* maquis declined,  
7 548 favouring the development of a Cistaceae-dominated shrubland. This forest dynamic may have been  
8 549 triggered either by land clearing practices of anthropogenic origin or by a climate change linked to the  
9 550 4.2 kyr BP event, corresponding to the Bond event 3 (Bond et al., 1997; Figure 11), but the evidence is  
10 551 too scanty to be attributable to one cause or the other. As there are no known Early Bronze Age sites  
11 552 in this area of Corsica, an anthropogenic origin for this sudden change in vegetation cover is therefore  
12 553 highly hypothetical. As for the 4.2 kyr BP event, this climate change does not appear to be associated  
13 554 to any general deforestation patterns in Corsica (Di Rita et al., 2022a, b). Conversely, several pollen  
14 555 sites show forest development (refs). We can therefore only speculate that an arid climate event, if  
15 556 one occurred, had only a limited impact on intermittent coastal ecosystems.  
16 557

17 558 *Roman times to the end of the Genoese period (2450-150 cal. BP/500 BCE-1800 CE)* - Mixed forests of  
18 559 *Pinus* and *Quercus ilex*, accompanied by maquis of *Erica* were the predominant component of the  
19 560 landscape until the change of era, when forest decline led to the expansion of maquis, predominated  
20 561 by *Erica* and with an increasing role of Cistaceae (Figs. 8 and 9). Until Roman times, human impact was  
21 562 limited in the evolution of forest cover in terms of short-term deforestation episodes and rapid  
22 563 recovery, consistent with previous studies in the area (Di Rita et al., 2022a). Only at Girolata can we  
23 564 report two brief episodes of forest decline dated at ca. 450 and 200 cal. BCE, mainly affecting the *Q.*  
24 565 *ilex* cover.

25 566 During Roman times (250 cal. BCE-400 cal. CE), the high values of *Quercus* suggest an expansion of oak  
26 567 forests in NW Corsica, possibly triggered by an increase in summer rainfall during the Roman Warm  
27 568 Period (RWP). These climate conditions also led to the development of freshwater swamps in the  
28 569 Girolata coastal plain (Figures 6 and 10). Subsequently, and following Roman Empire, deforestation  
29 570 processes and major changes in vegetation composition occurred. Indeed, from 500 CE onwards,  
30 571 regression of *Quercus* spp. values is evident in Girolata 2 and Fangu records, as is the decline of oak  
31 572 woods that began at the change of era in the area of Crovani and which is consolidated during this  
32 573 period. The Early Medieval cooling episode (500-900 cal. CE), also known as the Dark Ages or Migration  
33 574 Period Cooling (Ljungqvist, 2010) may be linked with this decline in oak woodland. This episode is  
34 575 clearly evidenced by minimum  $\delta^{18}O$  in GISP2 (Figure 13) and coincides with the 1.4 kyr cal. BP Bond  
35 576 event 1 (ca. 550 cal. CE; Bond et al., 1997), with RCC 1 (1.2-1.0 kyr cal. BP/750-950 cal. CE) defined in  
36 577 Mayewski et al. (2004). This period marked the transition from Late Antiquity to the Early Middle Ages  
37 578 when a strong human migration occurred in Europe between 300-700 cal. CE (Wanner et al., 2011).  
38 579 Finally, the strong human impact in the four pollen records during the first half of the second  
39 580 millennium CE (1000-1500 CE) leading to forest decline prevented from contrasting *Quercus* spp.  
40 581 curves with climate conditions from this phase onwards. Consequently, evidence from the NPPs record  
41 582 shows high concentrations of carbonicolous-lignicolous fungal spores in these chronologies in the  
42 583 Girolata pollen diagram (Figure 8) and numerous charcoals for Fangu core. These fires, associated to  
43 584 peaks in anthropogenic indicators, are interpreted as human-induced in other records (Lestienne et  
44 585 al., 2020; di Rita et al., 2022a), and explain the important role of fire in vegetation dynamics in the  
45 586 Mediterranean.  
46 587

### 47 588 5.3. Human impact on coastal landscape evolution of North-Western Corsica

48 589  
49 590 Figure 11 summarizes the recent pollen results acquired for four sites from the north western area of  
50 591 Corsica: published data from the Saint Florent and Crovani sites (Revelles et al., 2019; Di Rita et al.,

2022a) are combined with results obtained for the present study from the Fangu and Girolata sites. Arboreal pollens are associated with anthropogenic markers in order to evaluate the timing of human impact on the vegetation composition with a possible identification of climate control during Bond events.

### 5.3.1. For the UNESCO site (Fangu and Girolata coastal plains)

*Protohistory (Bronze Age: ca. 2200-800 cal. BCE)* – Evidence of human impact during the Bronze Age is scarce and is restricted to the southern part of the UNESCO site only, in the region of Girolata (Fig. 11). This site evidences agriculture during the Middle Bronze Age (1600-1350 cal. BCE, Phase 2; Figure 11), a period when the sites of human occupation (*I Casteddi/Castles*) were located primarily on the top of hill mounds or rocky outcrops (Pêche-Quilichini, 2015a and 2015b). Until now, no archaeological surveys confirming the presence of such a Middle Bronze Age site have been conducted in the UNESCO area, but in the near future archaeological prospections could include this cultural period and not only Medieval times. Cereal cultivation, though scarce, is attested during the Middle Bronze Age in the surroundings of the present day Girolata coastal plain. No indication of land-use is available for the Final Bronze Age (1200-800 cal. BCE) due to poor pollen preservation in the Girolata sequence, and to a lack of anthropogenic markers in the Fangu estuary area.

*Early Iron Age - Roman times (800 cal. BCE-500 cal. CE)* – Pollen results of both coastal sites clearly indicate that human activities have affected the vegetation composition for the previous 2000 years, and locally for the last 2500 years, with a significant and continuous impact on the forest cover starting from ca. 1650 cal. BP (300 cal. CE) and affecting both areas simultaneously. In addition, the Girolata 2 core shows evidence of agriculture during the whole Roman period (Phase 3; Figure 11), starting from ca. 450 cal. BCE to the 6<sup>th</sup> century CE with two intermittent phases of forest retreat dated ca. 450 and 200 cal. BCE. Two main agricultural phases can be distinguished (Figures 8 and 11): the first one dates from the 5<sup>th</sup> century BCE to the onset of the common era and combines both cereal cultivation and husbandry, as indicated by the presence of coprophilous fungi. The strong presence of *Vitis* during a short period of time over the Roman Republic (from ca. 500 to 350 cal. BCE; Figure 8) can be reasonably associated with grapevine cultivation on the hills surrounding the Girolata coastal wetland. The second phase ranges from the onset of the common era to the 6<sup>th</sup> century CE (Roman Empire) and is marked by a near-exclusive agricultural activity based on olive tree cultivation (*Olea* in Figure 8). At the onset of the common era, the sudden change in terms of land use around the Girolata coastal plain can be related to the major political changes that occurred in Rome during the transition from the Roman Republic to the start of the Roman Empire. The Roman Empire established a distinct specialisation concerning the type of agriculture undertaken in each province, a practice which can be inferred for Corsica, as well as in Northern Africa (Leveau, 1990). A clear and continuous agricultural activity is evidenced for the first time in Corsica in the Girolata sequence and in the vicinity of archaeological remains dating from throughout the Roman period (almost one millennium in duration). This confirms the geostrategic importance of both Girolata Bay and its coastal plain under the Roman domination of the Mediterranean. The Fangu site shows no clear human impact prior to the onset of the common era. The regression of pine forests and the progressive expansion of *Erica* maquis from 1600 cal. BP onwards (Figure 9) is best interpreted in the light of increasing human impact during Roman times, thus confirming Reille's vegetation pollen-based reconstruction (Reille, 1992a). However, the low resolution of the sequence pertaining to that period as well as the deposition of sands at 1.15-0.85m for the Fangu core make it difficult to study the socio-environmental dynamics during the Roman period.

1  
2  
3 639 *Late Antiquity, Medieval times, Pisan, and Genoese administrations of the island (500 cal. CE-Late*  
4 640 *18<sup>th</sup> century CE)* - At Fangu, Late Antiquity and the Medieval period correspond to phases of strong  
5 641 human impact on forest ecosystems of the island. The lowest values of arboreal pollen date to ca. 1150  
6 642 cal. CE and 1400 cal. CE, respectively (Figure 9), and reflect intense human activities during both the  
7 643 Pisan and Genoese administrations of the island. Forest decline during the Middle Ages was also  
8 644 reported at Crovani (Di Rita et al., 2022a; Fig. 1), situated only 6 km to the north, and at Saint Florent  
9 645 (Revelles et al., 2019). Reille's investigations at Fangu (Reille, 1992a) suggested that *Q. ilex* in the high  
10 646 Fangu valley probably replaced a burnt *P. laricio* forest around 1500 cal. BP. This anthropogenic  
11 647 disturbance mainly affected pine forests and *Erica* maquis, indicating deforestation processes both in  
12 648 the lowlands and uplands of the region. The presence of Cistaceae over the last 1500 years at Girolata  
13 649 (Figure 8) and over the last 1000 years at the Fangu site (Figure 9), combined with a high abundance  
14 650 of charcoal particles as observed and described during sedimentological analyses (no quantitative  
15 651 charcoal data are available at the moment) from ca. 1000 to 1500 cal. CE at the Fangu site reinforces  
16 652 the regular occurrence of fires within and in the vicinity of the UNESCO site. At Fangu, evidence of  
17 653 cereal cultivation is recorded solely during the Genoese administration of the island (Phase 4; Figure  
18 654 11), coeval with the building of the defensive towers during the 16<sup>th</sup> century CE in the vicinity of the  
19 655 Fangu estuary (Figs. 3A and 3B). Human disturbance probably explains the expansion of Mediterranean  
20 656 shrublands (*Erica*, Cistaceae, *Helianthemum-t*, *Ephedra*) and grasslands and ruderals (Poaceae,  
21 657 Asteraceae, *Plantago*; Fig. 9). The fact that no cereal cultivation is observed in the vicinity of the Fangu  
22 658 estuary prior the Genoese period reinforces the idea that this area was not of strategic interest for  
23 659 agricultural purposes, unlike the Girolata Plain which was certainly a major site in Corsica throughout  
24 660 Roman times.  
25 661

### 31 662 5.3.2. In NW Corsica: Nebbiu, Balagne and Filosorma areas

32 663 *Prehistory (Late to Final Neolithic times, 3900-2200 cal. BCE)* - Figure 11 shows evidence for agriculture  
33 664 and husbandry that points to an episode of human impact at the onset of the Late Neolithic (ca. 3900  
34 665 cal. BCE) in both Crovani and Saint Florent, with a limited impact on the forest cover (Human Impact  
35 666 (HI) episode 1; Figure 11). Following this, the Final Neolithic (2800-2200 cal. BCE) was a period of  
36 667 important agricultural development in NW Corsica, notably at Crovani (Di Rita et al., 2022a) and at  
37 668 Saint Florent (Revelles et al., 2019). Both of these sites record cereal cultivation and husbandry along  
38 669 the coastal zone within an environmental context of swampland, with a generally moderate impact of  
39 670 human activity on the forest cover (AP decline; Figure 11). It is noteworthy that a moderate forest  
40 671 decline is simultaneously observed at the onset of the Final Neolithic at Crovani and at Saint-Florent  
41 672 (ca. 2800-2600 cal. BCE, Phase 1; Figure 11), corresponding to a phase of agricultural development  
42 673 along the shoreline (Phase 1; Figure 11).  
43 674

44 675 *Protohistory (Bronze Age, 2200-800 cal. BCE)* - Following the Neolithic period, the Early Bronze Age  
45 676 shows little evidence of anthropogenic activities for NW Corsica, and this period is also largely marked  
46 677 by a paucity of sites of human occupation. In contrast, the period covering the Middle to Final Bronze  
47 678 Age (Phase 2, Figure 11) reveals a return to agricultural practices in the coastal areas at Girolata,  
48 679 Crovani and Saint Florent. A second phase of forest decline of moderate importance, consisting of  
49 680 short-term forest decline episodes followed by a rapid recovery, is observed during the Middle Bronze  
50 681 Age (Phase 2; Figure 12) which is a cultural period marked by the development of fortified castles (*/*  
51 682 *Casteddi*; Pêche-Quilichini, 2015b) on inland hilltops overhanging alluvial valleys (Ghilardi et al.,  
52 683 2017b). This type of site was clearly linked to isolated forest clearings and agricultural development,  
53 684 with grain storage inside the structures behind defensive walls. However, only low levels of cereal  
54 685 cultivation and scarce occurrences of husbandry are evidenced at Girolata (Phase 2, Figure 11), mainly  
55  
56  
57  
58  
59  
60



1  
2  
3 686 during the Middle Bronze Age. It seems that Fangu estuary was less favoured for agriculture at that  
4 687 time. The presence of the Fangu River associated with a flooding exposition of the area provides a  
5 688 reasonable explanation for such low agricultural activity in the lowlands  
6 689

7 690 *Early Iron Age - Roman times (800 cal. BCE-500 cal. CE)* – For the later Iron Age to Roman period, a  
8 691 major regional change with clear human impacts on the vegetation composition can be observed.  
9 692 During the Iron Age, evidence of cereal agriculture at Girolata and at Crovani, and probable *Vitis*  
10 693 cultivation around Girolata, are associated with moderate impact on forest cover (HI episode 2; Figure  
11 694 11). Agricultural development can thus be linked to a third phase of forest decline starting around the  
12 695 onset of the 5<sup>th</sup> century BCE at Girolata, Fangu and Crovani (Phase 3; Fig. 11), while forest decline in the  
13 696 area of Saint Florent appears approximately one millennium later (Figure 12). Similar observations of  
14 697 forest decline have also been reported for SW Corsica (Vella et al., 2019) and slightly earlier (2500  
15 698 years BP), on the Eastern coast (Currás et al., 2017), thus confirming Reille's conclusions concerning  
16 699 dating of the first important anthropogenic impacts on Corsican vegetation composition since the  
17 700 onset of Roman times (Reille, 1992a). Different dynamics are observed in Saint Florent and Girolata 2:  
18 701 human impact affected mainly *Alnus* spp. forests and to a lesser extent secondary pine forests (Revelles  
19 702 et al., 2019) in Saint Florent, but predominantly pine forests in Girolata (Figure 8). The Crovani record  
20 703 provides evidence of probable cultivation of olives during the Roman period (Di Rita et al., 2022a), a  
21 704 suggestion that may also be valid in the case of Girolata, where a peak of *Olea* led to a peak in the OVJC  
22 705 Index (Phase 3; Figure 11) during the Roman period. Anthropogenic activities during Roman times  
23 706 (Roman Republican) did not significantly affect forest cover or vegetation composition in general,  
24 707 whereas during the Roman Empire (at the onset of the common era) forest cover substantially  
25 708 declined.  
26 709

27 710 *Late Antiquity, Medieval times, Pisan and Genoese administrations of the island (500 cal. CE-Late*  
28 711 *18<sup>th</sup> century CE)* - From the pre-Christian era until the end of the Genoese administration of the island,  
29 712 human activities deeply impacted the pine forest (Phase 4; Figure 12). Reille (1992a) suggests that  
30 713 frequent fires burnt the *Pinus laricio*, a finding supported by our record from Fangu which reveals a  
31 714 large number of micro- and macro charcoals (not identified for the present study) in the 0.50-0.35 m  
32 715 depth range, roughly corresponding to the first half of the second millennium CE. To explain this  
33 716 decline, forest exploitation must also be examined through literary sources. Indeed, manuscripts  
34 717 dating from the Genoese administration of the island reveal that Corsican forests were exploited for  
35 718 their wood (see section 5.3.3. below). In addition, due to incursions of vandalism in the Corsican coastal  
36 719 areas and lowlands, the inhabitants were forced to migrate away from the coast and in doing so, the  
37 720 need for wood to build villages was substantial. The combination of forest exploitation and repeated  
38 721 fires provoked a rapid and strong reduction in forest cover during a period of political instability  
39 722 following Roman times.  
40 723

41 724 At the scale of the large Western Mediterranean islands, our results are consistent with palynological  
42 725 studies conducted on Minorca (Balearic Islands), where the Iron Age was a period of intense human  
43 726 activity and where landscape transformation during Roman times is evident in numerous records, such  
44 727 as at Algendar and Es Grau in Minorca (Yll et al., 1997; Burjachs et al., 2017). This is evidenced by the  
45 728 regression of AP, the expansion of maquis and the occurrence of *Cerealia-t*; and Prat de Vila (Ibiza;  
46 729 Burjachs et al., 2017), and also by the regression of pine forest, the expansion of maquis and  
47 730 grasslands, and the occurrence of *Cerealia-t*. In addition, on the Iberian Peninsula during the Roman  
48 731 period, large-scale deforestation resulted in open landscapes characterising lowland areas as a  
49 732 consequence of the intensification of human activities such as cropping, grazing, mining or forestry.  
50 733 Nevertheless, the decline of western Mediterranean forests, although initiated during the Roman

734 period, really began from the 10<sup>th</sup> century CE onwards (López-Sáez et al., 2015). Finally, the pollen  
 735 record of the Tirso coastal plain in Western Sardinia points to a clear open vegetation rich in  
 736 synanthropic herbs during the last millennium (Melis et al., 2017).

### 738 5.3.3. On the question of the exploitation of Corsican wood resources from Roman times onwards

739  
 740 Whereas archaeology has revealed little evidence regarding the exploitation of the forests of Corsica  
 741 during the historical period, the scrutiny of historical sources can provide precious information about  
 742 the exploitation of wood on the island (Rotta and Cancellieri, 2001). Indeed, the vegetation  
 743 reconstruction carried out in the UNESCO site for the present study has confirmed descriptions  
 744 recorded by ancient writers in documents spanning the last 2500 years.

745 The first event (Figure 12) of wood exploitation dates back to Early Roman times. The oldest  
 746 literary source to record this event can be found in descriptions made by Theophrastus (371-288 BCE),  
 747 who mentions an expedition for the recovery of wood. An attempt to build a city specialized in the  
 748 intermittent exploitation of the resource between 377 and 311 BCE was planned. Activities there  
 749 undoubtedly concerned the Laricio pine, defined by Teophrastus as “the largest of all” (*Historia*  
 750 *Plantarum*: V.8). This text reports the presence of many gulfs and shelters testifying to a high likelihood  
 751 that the later Roman expeditions most certainly took place on the western coast. During a short period  
 752 of time, the Romans deforested a large amount of wood in a "small area" a short distance from the  
 753 coast. The estimated date of the expedition fits tightly with the palynological results obtained for the  
 754 present study, which indicate significant human impact on forest cover, particularly in the area of  
 755 Girolata where pine forests regressed around 400 BCE (Figures 8, 11 and 12). It appears that this  
 756 exploitation was tied to the provisioning of materials for shipbuilding.

757 The second event also took place during the Roman Republic at around 200 BCE in the area of  
 758 Girolata, but no known ancient documents mention forest exploitation at that date.

759 The third event took place around the 4<sup>th</sup>-5<sup>th</sup> centuries CE (Figure 12). Victor de Vita writes in  
 760 about 486 CE (*History of the persecution of the Vandals*: V. 5) that a small number of Catholic bishops  
 761 from Africa were deported to the island for the exploitation of the forest. Despite the low number of  
 762 deportees mentioned, the pollen results agree with this historical fact and show the onset of a  
 763 deforestation process in the Fangu-Girolata area which also impacted oak forests (Figures 8, 9 and 11).

764 The fourth attested event of forest opening (Figure 12) took place during the first Muslim  
 765 invasions in the Mediterranean in around 717 CE when the Constantinople expedition was organized  
 766 in the quest for raw materials necessary for the construction of their fleets (Lombard, 1959 and 1972).  
 767 The search for sources of wood was persistent throughout the 9<sup>th</sup> and 10<sup>th</sup> centuries CE, and due to  
 768 clashes between the naval powers of the Caliphate and the Byzantine Empire, resources dwindled and  
 769 became the object of smuggling. As a direct consequence, Muslim invaders began to attack the coasts  
 770 of Anatolia, Dalmatia, Sardinia and Corsica (Lombard, 1972) in their search for wood. Strong evidence  
 771 of deforestation during this period is attested around Girolata, where the lowest AP values in the Late  
 772 Holocene in NW Corsica can be seen where human impact led to the abrupt regression of oak  
 773 woodlands and prevented the recovery of pine forests (Figure 8). In the case of Fangu, the decline of  
 774 arboreal pollen from 700 CE onwards coincides with the Muslim invasions, during which the majority  
 775 of wood exploitation focussed on pine forests (Figure 9). The Crovani area also experienced strong  
 776 forest decline during this period (Di Rita et al., 2022a), suggesting that the Girolata-Fangu-Crovani area  
 777 was regionally affected by forest clearance beginning in the 7<sup>th</sup>-8<sup>th</sup> centuries CE.

778 The fifth event can be observed during the Pisan and Genoese dominations of the island  
 779 between the 11<sup>th</sup> and 16<sup>th</sup> centuries CE (Figure 12). Archaeological data attest to changes in population  
 780 rhythms and settlement dynamics accompanied by a new colonization of spaces at the onset of the

1  
2  
3 781 2<sup>nd</sup> millennium CE (Mary, 2011, 2012, and 2020) when the demand for wooden constructions such as  
4 782 scaffolding, planks, beams and frames became significant. The Pisan colonization of the island (1070-  
5 783 1284 CE) required that certain areas be cleared to permit cultivation of the land: the forest cover  
6 784 therefore underwent a strong decline. This is revealed by the pollen diagrams from both Girolata Plain  
7 785 (Figure 8) and the Fangu estuary (Figure 9), with additional forest regression attested in Crovani and  
8 786 Saint Florent in the same chronologies (Phase 4, Figure 11). During this period, strong evidence of  
9 787 farming activities is documented in the area of Girolata, with high values of cereal pollen and  
10 788 coprophilous fungi suggesting the practice of animal husbandry in the surrounding areas (Figures 8 and  
11 789 11). At the beginning of the 16<sup>th</sup> century CE (1510 CE), the Republic of Genoa took full possession of  
12 790 the island and the generalised exploitation of the island's forests began. This supports the fourth phase  
13 791 of human impact and deforestation as defined by pollen analysis (Figures 11 and 12). The impact of  
14 792 farming activities during this period is also attested in the Fangu area (Figure 9), suggesting  
15 793 demographic growth or expansion of human communities in the territory. The Office of Saint Georges  
16 794 of the Genoese Republic established the first project (Della Grossa et Montegiani, 2016), including the  
17 795 western coast of Corsica which was the most popular region according to descriptions recorded by  
18 796 Monsignor Giustiniani (Giustiniani, 1993), who also mentions that the wood from the mountain sector  
19 797 surrounding Galeria was transported to the coast and that the inhabitants of Calvi traded it both  
20 798 domestically and off-island. The full development of wood exploitation was set up in the 17<sup>th</sup> century  
21 799 CE with the development of inland exploitation at Aitone or Guagno where the trees were older,  
22 800 straighter, taller, and of a higher quality, according to the Dutch captain Cornelius de Witt who was  
23 801 dispatched there by the Genoese in 1639 (Archivio di stato di Genova, 1639). This development  
24 802 towards the exploitation of the island's interior woodlands is a clear example of landscape degradation  
25 803 through the intensive exploitation of NW Corsican coastal forests which took place during the Middle  
26 804 Ages and early Modern Age. Similarly, this shift toward inland resources may also explain the coastal  
27 805 forest recovery attested in pollen diagrams for the area of Fangu and Crovani from 1600 CE onwards  
28 806 (Figure 12).

807

## 36 808 **6. Conclusions**

37 809 The multidisciplinary dataset obtained for both the UNESCO site of Scandola-Galeria and the NW area  
38 810 of the Corsican regional park helps to reconstruct past human-environment interactions over the last  
39 811 six millennia for the first time. The main outcomes of the present work are summarized as follows:

42 812 1. The coastal plains of Girolata and Fangu formed at different times: formation of the Fangu  
43 813 deltaic plain began around 3500 cal. BCE following the "classical" scenario observed for most  
44 814 of the large Mediterranean deltas. The Girolata coastal plain is much younger and mainly  
45 815 formed from the mid-second millennium BCE to the mid-first millennium BCE. The Girolata  
46 816 plain formation shows similar features with nearby deltaic plains such as at Sagone, situated  
47 817 ca. 25 km southwards (Figure 12) and the coastal plains of Tuscany (Ombrone and Magra  
48 818 Rivers) and Latium (Tiber River).

49 819 2. The northern part of the UNESCO site (Fangu estuary) is scarcely affected by anthropogenic  
50 820 activities until the mid-first millennium CE, while the southern part (Girolata coastal plain)  
51 821 records human impacts on the vegetation composition beginning in approximately the Mid-  
52 822 first millennium BCE, corresponding to the onset of the Roman Republic. Before any human  
53 823 impact, forest vegetation composition was characterised by the predominance of a dense  
54 824 maquis with predominance of *Erica* sp. in the coastal area, as was recorded by Maurice Reille,  
55 825 and which has also recently been confirmed by the pollen-based vegetation reconstructions  
56 826 for the nearby Crovani (Di Rita et al., 2022a) and Saint Florent (Revelles et al., 2019) areas.

- 1  
2  
3 827 3. The Girolata Plain and its surroundings was an important site of human occupation during  
4 828 Roman times from the 5<sup>th</sup> century BCE until the 6<sup>th</sup> century CE, and benefitted from favourable  
5 829 environmental conditions for the development of agriculture, with the presence of a  
6 830 freshwater swamp throughout Roman times. It is clear that the sheltered bay of Girolata  
7 831 served as a natural harbour for the importation of goods for approximately one millennium.  
8 832 Evidence of land use in the environs of the Girolata Plain reveals the presence of agricultural  
9 833 communities who first practiced cereal cultivation and viticulture alongside livestock breeding  
10 834 during the first phase of Roman times (5<sup>th</sup> century BCE-1<sup>st</sup> century CE, Roman Republic), and  
11 835 who then developed a dominant *Olea* cultivation which superseded cereal cultivation and  
12 836 livestock breeding during the second phase (1<sup>st</sup>-6<sup>th</sup> centuries CE, Imperial Period). The Girolata  
13 837 pollen sequence is one of the rare Corsican, and even western Mediterranean sequences, to  
14 838 fully reconstruct human impacts (including land-use practices) on the vegetation composition  
15 839 throughout Roman times. To the north, in the Fangu catchment, a period of reinforced alluvial  
16 840 activity is observed throughout Roman times and may be explained by changes in land-use in  
17 841 the uplands related to the Girolata inland forest exploitation. Further palynological  
18 842 investigations will undoubtedly provide more accurate documentation of vegetation  
19 843 composition in the northern area of the UNESCO site during Roman times.
- 20 844 4. The UNESCO site began to be affected by the strong impact of human activities from the mid-1<sup>st</sup>  
21 845 millennium CE, with significant and widespread clearing of upland pine forests and lowland  
22 846 maquis starting in Roman times. Potential upland forest clearance may have provoked  
23 847 reinforced alluvial activity of the Fangu River during the Roman Warm Period (RWP),  
24 848 characterized by regionally wet climate conditions. The substantial reductions of forest cover  
25 849 were greatest during the Middle Ages, when pollen records indicate the lowest cover over the  
26 850 past four millennia, and throughout the Pisan-Genoese administration of the island,  
27 851 confirming regional observations made to the north and northeast in the Crovani and Saint  
28 852 Florent areas, respectively. Wood resources were intensely exploited during the Pisan-  
29 853 Genoese colonization of Corsica leading to minimum expansion of the woodland during the  
30 854 Late Holocene.
- 31 855 5. Vegetation changes represented by the replacement of *Erica*-dominated maquis by Cistaceae-  
32 856 dominated shrubland is recorded in the Fangu pollen record and may be linked either to  
33 857 human activities or to local effects of the 4.2 kyr cal. BP climate event (Bond event 3).
- 34 858 6. Detrital input is recorded at ca. 3.2 kyr cal. BP and reveals a possible climate control on the  
35 859 sediment dynamics of the local streams, related to the 3.2 kyr cal. BP RCC event. This event is  
36 860 also evidenced for several coastal plains situated on the western coast of Corsica and around  
37 861 the Gulf of Lion.
- 38 862 7. The 2.8 kyr cal. BP event (Bond event 2, Homeric Minimum) has been hypothesised as a driving  
39 863 factor of a phase of major fluvial input recorded in the Girolata area, and is also probably linked  
40 864 to a shoreline progradation pattern at regional scale.  
41 865

### 866 Funding and acknowledgements

867 The studies at Girolata and Fangu were undertaken in 2020 and 2021, respectively, within the  
868 framework of the PhD thesis of Jean-Baptiste Mary (University of Lyon II/Collectivité de Corse). This  
869 article is a contribution to the PCR "Approche géoarchéologique des paysages de Corse à l'Holocène,  
870 entre mer et intérieur des terres « Tra Mare à Monti »" programme (2018-2020), funded by the DRAC  
871 Corsica (Ministry of Culture) and directed by Matthieu Ghilardi. The Regional Park of Corsica is  
872 acknowledged for providing substantial field assistance during coring campaigns. The authors are  
873 grateful to Jean-François Luciani for his precious help during summer 2020 fieldwork in Girolata.

874 Jordi Revelles is a member of the GAPS (2017 SGR 836) research group and acknowledges postdoctoral  
 875 fellowship support from the Spanish “Juan de la Cierva Incorporación (IJC2020)” program (MICINN,  
 876 Spain). The Institut Català de Paleoecologia Humana i Evolució Social (IPHES-CERCA) received financial  
 877 support from the Spanish Ministry of Science and Innovation through the “María de Maeztu” program  
 878 for Units of Excellence (CEX2019-000945-M). This paper is also a contribution to the "HumAN and  
 879 climAtic iMPlicatioNs of palaEoecological changeS in large ISlands in the central Mediterranean  
 880 (ANAMNESIS, Code: RM1221816B963D12, University of Roma La Sapienza)" programme directed by  
 881 Federico Di Rita. The authors also acknowledge Pr. V. Pascucci and an anonymous reviewer for their  
 882 fruitful comments. Finally, we would like to thank Rachel Mackie for improving the English.

883

884 **References**

885 Archivio di stato di Genova, 1639. Cornelius de Witt: source archivistique, fond Corsica, 948, Relatione del bosco  
 886 di Aitona del Capitano Olandese.

887  
 888 Bassetti MA, Berné S, Sicre, MA, Dennielou B, Alonso Y, Buscail R, Jalali B, Herbert B, Menniti C (2016)  
 889 Holocene hydrological changes in the Rhône River (NW Mediterranean) as recorded in the marine mud belt.  
 890 *Climate of the Past* 12: 1539-1553.

891  
 892 Bengtsson L, Enell M (1986) Chemical analysis. In: Berglund BE (Ed.), *Handbook of Holocene Palaeoecology*  
 893 *and Palaeohydrology*. John Wiley & Sons Ltd., Chichester, 423-451.

894  
 895 Berger JF, Brochier JL, Vital J, Delhon C, Thiebault S (2007) Nouveau regard sur la dynamique des paysages et  
 896 l'occupation humaine à l'Âge du bronze en moyenne vallée du Rhône. In : Mordant C, Richard H, Magny M (eds),  
 897 *Environnements et cultures à l'âge du Bronze en Europe occidentale*. Actes du 129e colloque du CTHS, Besançon,  
 898 avril 2004, Editions du CTHS, Documents Préhistoriques, 21, 260-283.

899  
 900 Biserni G and van Geel B (2005) Reconstruction of Holocene palaeoenvironment and sedimentation history of the  
 901 Ombrone alluvial plain (South Tuscany, Italy). *Review of Palaeobotany and Palynology* 136(1-2): 16-28.

902  
 903 Blaauw M (2010) Methods and code for ‘classical’ age-modelling of radiocarbon sequences. *Quat Geochronol* 5  
 904 : 512–518.

905  
 906 Bond G, Showers W, Cheseby M, Lotti R, Almasi P, deMenocal PB, Priore P, Cullen H, Hajdas I, Bonani G (1997)  
 907 A pervasive millennial-scale cycle in North Atlantic Holocene and glacial climates. *Science* 278 : 1257–1265.

908  
 909 Brisset E, Burjachs F, Ballesteros Navarro BJ, Fernández-López J (2018). Socioecological adaptation to Early-  
 910 Holocene sea-level rise in the western Mediterranean. *Global and Planetary Change* 169: 56-167.

911  
 912 Brückner H, Vött A, Schriever A, Handl M (2005) Holocene delta progradation in the eastern Mediterranean— case  
 913 studies in their historical context. *Méditerranée* 104 : 95-106.

914  
 915 Burjachs F, Jones SE, Giralt S, de Pablo JFL (2016) Lateglacial to Early Holocene recursive aridity events in the  
 916 SE Mediterranean Iberian Peninsula: The Salines playa lake case study. *Quaternary International* 403: 187-200.

917  
 918  
 919 Burjachs F, Pérez-Obiol R, Picornell-Gelabert L, Revelles J, Servera-Vives G, Expósito I, Yll EI (2017) Overview  
 920 of environmental changes and human colonization in the Balearic Islands (Western Mediterranean) and their  
 921 impacts on vegetation composition during the Holocene. *Journal of Archaeological Science: Reports*: 12: 845-859.

922  
 923 Buurman P, Pape T, Muggler CC (1996) Laser grain-size determination in soil genetic studies: practical problems.  
 924 *Soil Sci.* 162 (3) : 211–218.

925  
 926 Cacho I, Grimalt JO, Canals M, Sbaiffi L, Shackleton NJ, Schoenfeld J, Zahn R (2001) Variability of the western  
 927 Mediterranean Sea surface temperature during the last 25,000 years and its connection with the Northern  
 928 Hemisphere climatic changes. *Paleoceanography* 16 (1): 40-52.

- 929  
930 Català A, Cacho I, Frigola J, Pena L D, Lirer F (2019). Holocene hydrography evolution in the Alboran Sea: a  
931 multi-record and multi-proxy comparison. *Climate of the Past*15(3) : 927-942.  
932  
933 Cibecchini F, Dieulefet G (2014) Le site de mouillage de Girolata (Corse). *Archéothème* 32 : 16-19.  
934  
935 Currás A, Ghilardi M, Peche-Quilichini K, Fagel N, Vacchi M, Delanghe D, Contreras D, Vella C, Ottaviani, JC  
936 (2017). Reconstructing past landscapes of the eastern plain of Corsica (NW Mediterranean) during the last 6000  
937 years based on molluscan, sedimentological and palynological analyses. *J. Archaeol. Sci.: Report* 12: 755-769.  
938  
939 Dean Jr. W.E (1974) Determination of carbonate and organic matter in calcareous sediments and sedimentary  
940 rocks by loss on ignition: comparison with other methods. *J. Sediment. Petrol.* 44: 242-248.  
941  
942 Della Grossa G. et Montegiani P. 2016. *Giovanni Della Grossa, Pier'Antonio Montegiani. Chronique de la Corse*  
943 *des origines à 1546. Introduction, traduction et notes d'Antoine-Marie Graziani, Ajaccio, Piazzola, 592-593.*  
944  
945 Di Rita F, Magri D (2012) An overview of the Holocene vegetation history from the central Mediterranean coasts.  
946 *J. Mediterr. Earth Sci.* 4: 35-52.  
947  
948 Di Rita F, Ghilardi M, Fagel N, Vacchi M, Warichet F, Delanghe D, Sicurani J, Martinet L, Robresco S (2022a).  
949 Natural and anthropogenic dynamics of the coastal environment in north western Corsica (Western Mediterranean)  
950 over the past six millennia. *Quaternary Science Reviews* 278: 107372  
951  
952 Di Rita F, Michelangeli F, Celant A, Magri D (2022b) Sign-switching ecological changes in the Mediterranean  
953 basin at 4.2 ka BP. *Global and Planetary Change* 208: 103713.  
954  
955 Emberger L (1930) La végétation de la région méditerranéenne: essai d'une classification des groupements  
956 végétaux. *Revue de Botanique*, Librairie générale de l'enseignement, 503: 642-662 ; 504:705-721.  
957  
958 Faegri K, Iversen J (1989) *Text-book of modern pollen analysis*. Ejnar Munksgaard. Copenhagen.  
959  
960 Fletcher WJ, Debret M, Goñi MFS (2013) Mid-Holocene emergence of a low-frequency millennial oscillation in  
961 western Mediterranean climate: Implications for past dynamics of the North Atlantic atmospheric westerlies. *The*  
962 *Holocene* 23 (2) : 153-166.  
963  
964 Fontana A, Vinci G, Tasca G, Mozzi P, Vacchi M, Bivi G, Salvador S, Rossato S, Antonioli F, Asioli A, Bresolin  
965 M, Di Mario F, Hajdas I (2017) Lagoonal settlements and relative sea level during bronze age in northern Adriatic:  
966 Geoarchaeological evidence and paleogeographic constraints. *Quat. Int.* : 439 : 17-36.  
967  
968 Galop D, Carozza L, Marembert F, Bal MC (2007) Activités agropastorales et climat durant l'Âge du Bronze dans  
969 les Pyrénées : l'état de la question à la lumière des données environnementales et archéologiques. In : Mordant C,  
970 Richard H, Magny M. (eds) *Environnements et cultures à l'âge du Bronze en Europe occidentale*. Actes du 129e  
971 colloque du CTHS, Besançon, avril 2004, Editions du CTHS, Documents Préhistoriques, 21, 107-119.  
972  
973 Ghilardi M (2021) Geoarchaeology: where Geosciences meet with Humanities to reconstruct past  
974 Humans/Environment interactions. An application to the coastal areas of the largest Mediterranean islands.  
975 *Applied Sciences* 11 (10): 4480.  
976  
977 Ghilardi M (2020) *Lagunes et marais littoraux de Corse. De la Préhistoire à nos jours*. Collec. Orma : la Corse  
978 archéologique, Editions ARAC, 5 : 105 p.  
979  
980 Ghilardi M, Istria D, Currás A, Vacchi M, Contreras D, Vella C, Dussouillez P, Crest Y, Colleu M, Guiter F,  
981 Delanghe D. (2017a) Reconstructing the landscape evolution and the human occupation of the Lower Sagone  
982 River (Western Corsica, France) from the Bronze Age to the Medieval period. In: Ghilardi M and Lespez L (eds),  
983 *Geoarchaeology of the Mediterranean islands*, Journal of Archaeological Science: Reports, 12: 741-754.  
984  
985 Ghilardi M, Delanghe D, Demory F, Leandri F, Pêche-Quilichini K, Vacchi M, Vella MA, Rossi V, Robresco S  
986 (2017b) Enregistrements d'événements extrêmes et évolution des paysages dans les basses vallées fluviales du  
987 Taravo et du Sagone (Corse occidentale, France) au cours de l'âge du Bronze moyen à final : une perspective  
988 géoarchéologique. *Géomorphologie, Relief, Processus et Environnement* 23(1) : 15-35.

- 1  
2  
3 989  
4 990 Giaime M, Salem A, Wang Y, Zhao X, Liu Y, Chen J, Sun A, Abu Shama AM, Elhossainy M, Morhange C, Chen  
5 991 Z (2022). Holocene evolution and signature of environmental change of the Burullus lagoon (Nile Delta)  
6 992 deciphered from a long sediment record. *Palaeogeography, Palaeoclimatology, Palaeoecology* 590 : 110861.  
7 993  
8 994 Girard M, Renault-Miskovsky J (1969) Nouvelles techniques de préparation en Palynologie appliqués à trois  
9 995 sédiments du Quaternaire final de l'Abri Cornille (Istres -Bouches du Rhône). *Bulletin AFEQ* 4: 275-284.  
10 996  
11 997 Giraudi C (2011) The sediments of the "Stagno di Maccarese" marsh (Tiber river delta, central Italy): A late-  
12 998 Holocene record of natural and human-induced environmental changes. *The Holocene* 21(8): 1233-1243.  
13 999  
14 1000 Giraudi C, Tata C, Paroli L (2009) Late Holocene evolution of the Tiber river delta and geoarchaeology of Claudius  
15 1001 and Trajan harbour, Rome. *Geoarchaeology* 24(3) : 371-382.  
16 1002  
17 1003 Giustiniani A., 1993. *Augustino Giustiniani. Description de la Corse. Préface, notes et traduction d'Antoine-*  
18 1004 *Marie Graziani.* Ajaccio, Piazzola, coll. Source de l'Histoire de la Corse, Textes et documents.  
19 1005  
20 1006 Goeury C, de Beaulieu JL (1979) À propos de la concentration du pollen à l'aide de la liqueur de Thoulet dans les  
21 1007 sédiments minéraux. *Pollen et Spores* XXI (1-2): 239- 251.  
22 1008  
23 1009 Graziani A.M., 2004. *La forêt en Corse. Des origines à nos jours*, Archives départementales de la Corse-du-Sud,  
24 1010 Ajaccio, 59 p.  
25 1011  
26 1012 Grimm EC (1987) CONISS: a Fortran 77 program for stratigraphically constrained cluster analysis by the method  
27 1013 of incremental sum of squares. *Comput.Geosci.* 13:13-55.  
28 1014  
29 1015 Grimm EC (1991-2011). Tilia, Tilia-Graph and TGView. Illinois State Museum, Springfield,  
30 1016 <http://museum.state.il.us/pub/grimm/tilia/>  
31 1017  
32 1018 Huser A, Ben Chaba L, Abel V, Sivan O (2017). *Le fortin de Girolata. Une tour isolée devenue fortin, fouille et*  
33 1019 *étude du bâti.* Rapport final de synthèse (INRAP), Nîmes, 444pp.  
34 1020  
35 1021 Lestienne M, Jouffroy-Bapicot I, Leysenne D, Sabatier P, Debret M, Albertini PJ, Colombaroli D, Didier J, Hély  
36 1022 C, Vannière B (2020). Fires and human activities as key factors in the high diversity of Corsican vegetation. *The*  
37 1023 *Holocene* 30: 244-257.  
38 1024  
39 1025 Leveau P (1990) L'organisation de l'espace agricole en Afrique à l'époque romaine. In : L'Afrique dans l'Occident  
40 1026 romain (Ier siècle av. J.-C. - IVe siècle ap. J.-C.). Actes du colloque de Rome (3-5 décembre 1987) Rome : École  
41 1027 Française de Rome, *Publications de l'École française de Rome*, 134 : 129-141.  
42 1028  
43 1029 Leys B, Finsinger W, Carcaillet C (2014) Historical range of fire frequency is not the Achilles' heel of the Corsican  
44 1030 black pine ecosystem. *Journal of Ecology* 102(2): 381–395.  
45 1031  
46 1032 Leys B, Curt T, Elkin C (2018) Mosaic landscape pattern explains vegetation resistance to high fire frequency in  
47 1033 Corsica over the last six millennia. *Int J Earth Sci Geophys* 4: 1-7.  
48 1034  
49 1035 Lombard M (1959) Un problème cartographié : le bois dans la Méditerranée musulmane: VIIe-XIe siècles. Armand  
50 1036 Colin, *Annales Economie-Sociétés-Civilisations* 2 : 234-254.  
51 1037  
52 1038 Lombard M (1972) Espaces et réseaux du haut moyen âge, Mouton, Paris : École des Hautes Études en Sciences  
53 1039 Sociales, coll. « *Le savoir historique 2* » : 162-165.  
54 1040  
55 1041 López-Belzunce M, Blázquez AM, Carmona P, Ruiz JM (2020). Multi proxy analysis for reconstructing the late  
56 1042 Holocene evolution of a Mediterranean Coastal Lagoon: Environmental variables within foraminiferal  
57 1043 assemblages. *Catena* 187: 104333.  
58 1044  
59 1045 López-Sáez JA, Pérez-Díaz S, Galop D, Alba-Sánchez F, Abel-Schaad D (2015) A Late Antique vegetation history  
60 1046 of the Western Mediterranean in context. *Late Antique Archaeology* 11(1): 83-104.  
61 1047

- 1  
2  
3 1048 Ljungqvist F.K. (2010) A new reconstruction of temperature variability in the extra-tropical northern hemisphere  
4 1049 during the last two millennia. *Geografiska Annaler : Series A, Physical Geography* 92(3), 339-351.  
5 1050
- 6 1051 Magny M (2004) Holocene climate variability as reflected by mid-European lake level fluctuations and its probable  
7 1052 impact on prehistoric human settlements. *Quaternary International* 113: 65-79.  
8 1053
- 9 1054 Magny M, de Beaulieu JL, Drescher-Schneider R, Vanni re B, Walter-Simonnet AV, Miras Y, Millet L, Bossuet  
10 1055 G, Peyron O, Brugiapaglia E, Leroux A (2007). Holocene climate changes in the central Mediterranean as recorded  
11 1056 by lake-level fluctuations at Lake Accesa (Tuscany, Italy). *Quaternary Science Reviews* 26(13-14): 1736-1758.  
12 1057
- 13 1058 Marco-Barba J, Holmes JA, Mesquita-Joanes F, Miracle MR (2013) The influence of climate and sea-level change  
14 1059 on the Holocene evolution of a Mediterranean coastal lagoon: Evidence from ostracod palaeoecology and  
15 1060 geochemistry. *Geobios* 46(5): 409-421.  
16 1061
- 17 1062 Marco-Barba J, Burjachs F, Reed JM, Santisteban C, Usera JM, Alberola C, Exposito I, Guillem J, Patchett F,  
18 1063 Mesquita-Joanes F, Miracle MR (2019) Mid-holocene and historical palaeoecology of the albufera de Val ncia  
19 1064 Coastal Lagoon. *Limnetica* 38 : 353-389.  
20 1065
- 21 1066 Mary JB (2013) *Analyses et approches typologiques de l'occupation protohistorique et antique de la r gion ouest*  
22 1067 *de la Corse*. Master thesis, University of Aix-Marseille, 160 p.  
23 1068
- 24 1069 Mary JB (2014a) *Nouveau regard sur les fortifications de l' ge du Fer au changement d' re : le cas de la fa ade*  
25 1070 *centre occidentale*. Master Thesis, University of Aix-Marseille, 189 p.  
26 1071
- 27 1072 Mary JB (2014b) *Prospection-inventaire des communes de Partinellu, Ota et Osani*. Rapport final de Synth se,  
28 1073 Service R gional de l'Arch ologie de Corse, 10-27.  
29 1074
- 30 1075 Mary JB (2014c) * tude du mobilier c ramique du fortin de Girolata*. In : le fortin de Girolata, Rapport d'op ration  
31 1076 (INRAP), N mes, 104-111.  
32 1077
- 33 1078 Mary JB (2018)  tudes et constat pr liminaires des implantations fortifi es de Corse, du second  ge du Fer au  
34 1079 changement d' re. Le cas de la r gion centre-ouest de la Corse. In : *insularity and identity in the Roman*  
35 1080 *Mediterranean*, Oxbow books :165-198.  
36 1081
- 37 1082 Mary JB (2021) *Prospection-th matique avec sondages d' valuation, 2020. Communes de Coggia, Vico, Carg se,*  
38 1083 *Piana, Ota, Serierra, Partinellu, Osani (Corse-du-Sud)*. Rapport final de synth se, Service r gional de  
39 1084 l'arch ologie de Corse, 164 p.  
40 1085
- 41 1086 Mary JB (2022) * tude du mobilier c ramique du fortin de Girolata*. In : le fortin de Girolata, Rapport d'op ration  
42 1087 (INRAP), N mes, 127-137.  
43 1088
- 44 1089 Mayewski PA, Rohling EE, Stager JC, Karlen W, Maasch KA, Meeker LD, Meyerson EA, Gasse F, Van Kreveld  
45 1090 S, Holmgren K, Lee-Thorp J, Rosqvist G, Rack F, Staubwasser M, Schneider RR, Steig EJ (2004) Holocene  
46 1091 climate variability. *Quaternary Research* 62 (3): 243-255.  
47 1092
- 48 1093 Melis RT, Depalmas A, Di Rita F, Montis F, Vacchi M (2017) Mid to late Holocene environmental changes along  
49 1094 the coast of western Sardinia (Mediterranean Sea). *Global and Planetary Change* 155 : 29-41.  
50 1095
- 51 1096 Pascucci V., De Falco G., Del Vais C., Sanna I., Melis R.T., Andreucci S. (2018) Climate changes and human  
52 1097 impact on the Mistras coastal barrier system (W Sardinia, Italy), *Marine Geology* 395 : 271-284.  
53 1098
- 54 1099 P che-Quilichini K (2015a) Les torre. Enigmatiques tours de l' ge du Bronze. *Archaeologia* 528 : 49-55.  
55 1100
- 56 1101 P che-Quilichini K (2015b) L' ge du Bronze corse. L' mergence d'une  lite guerri re. *Dossiers d'Arch ologie*  
57 1102 370: 24-29.  
58 1103
- 59 1104 P res JM (1982) Major benthic assemblages. In: Kinne O (ed), *Marine Ecology*, Part 1, vol. 5. Wiley, Chichester,  
60 1105 pp. 373-522.  
61 1106



- 1  
2  
3 1107 Pères JM, Picard J (1964). Nouveau manuel de Bionomie benthique de la Mer Méditerranée. *Recueil des Travaux*  
4 1108 *de la station Marine d'Endoume*31 (47) : 5-137.  
5 1109  
6 1110 Petti Balbi G (1976) *Genova nel trecento*, 97-98. Istituto storico italiano per il medio evo, Roma, 195 p.  
7 1111  
8 1112 Poher Y, Ponel P, Médail F, Andrieu-Ponel V, Guiter F (2017) Holocene environmental history of a small  
9 1113 Mediterranean island in response to sea-level changes, climate and human impact. *Palaeogeography,*  
10 1114 *Palaeoclimatology, Palaeoecology* 465: 247-263. Part A.  
11 1115  
12 1116 Pranzini E (2001) Updrift river mouth migration on cusped deltas : two examples from the coast of Tuscany  
13 1117 (Italy). *Geomorphology* 38: 125-132.  
14 1118  
15 1119 Rasmussen SO, Bigler M, Blockley SP, Blunier T, Buchardt SL, Clausen HB, Cvijanovic I, Dahl-Jensen D,  
16 1120 Johnsen SJ, Fischer H, Gkinis V, Guillevic M, Hoek WZ, Lowe JJ, Pedro JB, Popp T, Seierstad IK, Steffensen JP,  
17 1121 Svensson AM, Vallelonga P, Vinther BM, Walker MJC, Wheatley JJ, Winstrup M (2014) A stratigraphic  
18 1122 framework for abrupt climatic changes during the Last Glacial period based on three synchronized Greenland ice-  
19 1123 core records: refining and extending the INTIMATE event stratigraphy. *Quat. Sci. Rev.* 106: 14–28.  
20 1124  
21 1125 Reille M (1992a) New pollen-analytical researches in Corsica: the problem of *Quercus ilex* L. and *Erica arborea*  
22 1126 L., the origin of *Pinus halepensis* Miller forests. *New Phytologist* 122: 359-378.  
23 1127  
24 1128 Reille M(1992b) *Pollen et spores d'Europe et d'Afrique du nord, Laboratoire de botanique historique et*  
25 1129 *palynologie*. Marseille, France: URA, CNRS, Laboratoire de Botanique Historique et Palynologie.  
26 1130  
27 1131 Reille M (1988) Recherches pollenanalytiques dans le cap Corse: analyse pollinique du marais de Barcaggio. *Trav.*  
28 1132 *Sci. du Parc Nat. régional des Réserves Nat. Corse* 18 : 77-92.  
29 1133  
30 1134 Reille M (1984) Origine de la végétation actuelle de la Corse sud-orientale; analyse pollinique de cinq marais  
31 1135 côtiers. *Pollen et Spores* 26 : 43-60.  
32 1136  
33 1137 Reille M (1975) *Contribution pollenanalytique à l'histoire tardiglaciaire et holocène de la végétation de la*  
34 1138 *montagne corse*. Thèse de Doctorat des sciences, Aix-Marseille III.  
35 1139  
36 1140 Reimer PJ and McCormac FG (2002) Marine radiocarbon reservoir corrections for the Mediterranean and Aegean  
37 1141 Seas. *Radiocarbon* 44 (1) :, 159-166.  
38 1142  
39 1143 Reimer P, Austin WEN, Bard E, Bayliss A, Blackwell PG, Bronk Ramsey C, Butzin M, Cheng H, Edwards RL,  
40 1144 Friedrich M, Grootes PM, Guilderson TP, Hajdas I, Heaton TJ, Hogg AG, Hughen KA, Kromer B, Manning SW,  
41 1145 Muscheler R, Palmer JG, Pearson C, van der Plicht J, Reimer RW, Richards DA, Scott EM, Southon JR, Turney  
42 1146 CSM, Wacker L, Adolphi F, Büntgen U, Capano M, Fahrni S, Fogtmann-Schulz A, Friedrich R, Köhler P, Kudsk  
43 1147 S, Miyake F, Olsen J, Reinig F, Sakamoto M, Sookdeon A, Talamo S (2020)The IntCal20 Northern Hemisphere  
44 1148 radiocarbon age calibration curve (0-55 calkBP). *Radiocarbon* 62(4):725-757.  
45 1149  
46 1150 Revelles J, Ghilardi M, Vacchi M, Rossi V, Currás A, López-Bultò O, Brkojewitsch G (2019) Coastal landscape  
47 1151 evolution of Corsica: palaeoenvironments, vegetation history and human impacts since the Early Neolithic period,  
48 1152 *Quaternary Science Reviews*, 105993.  
49 1153  
50 1154 Revelles J, Burjachs F, Van Geel B (2016) Pollen and non-pollen palynomorphs from the Early Neolithic  
51 1155 settlement of La Draga (Girona, Spain). *Review of Palaeobotany and Palynology* 225: 1-20.  
52 1156  
53 1157 Rotta MP and Cancellieri JA (2001) *De la nature à l'histoire; les forêts de la Corse*. Ed. Alain Piazzola, 159 p.  
54 1158  
55 1159 Sabatier P, Dézileau L, Barbier M, Raynal O, Lofi J, Briquieu L, Condomines M, Bouchette F, Certain R, Van  
56 1160 Grafenstein U, Jorda C, Blanchemanche P (2010). Late-Holocene evolution of a coastal lagoon in the Gulf of  
57 1161 Lions (South of France). *Bulletin de la Société géologique de France* 181 (1) : 27-36.  
58 1162  
59 1163 Servera-Vives G, Riera S, Picornell-Gelabert L, Moffa-Sánchez P, Llergo Y, Garcia A, ... &Trías MC (2018). The  
60 1164 onset of islandscapes in the Balearic Islands: A study-case of Addaia (northern Minorca, Spain). *Palaeogeography,*  
61 1165 *Palaeoclimatology, Palaeoecology*498: 9-23.  
62 1166

- 1  
2  
3 1167 Shom - Collectivité de Corse - Dreal Corse (2020)*Litto3D*,  
4 1168 [https://dx.doi.org/10.17183/L3D\\_MAR\\_CORSE\\_2017\\_2018](https://dx.doi.org/10.17183/L3D_MAR_CORSE_2017_2018)  
5 1169  
6 1170 Siani G, Paterne M, Arnold M, Bard E, Metivie B, Tisnerat N, Bassinot F (2000) Radiocarbon reservoir ages in  
7 1171 the Mediterranean Sea and Black Sea. *Radiocarbon* 42 : 271–280.  
8 1172  
9 1173 Stuiver M and Reimer P.J (1993) Calib software v. 8.2, *Radiocarbon* 35 : 215-230.  
10 1174  
11 1175 Tramoni P, d'Anna A (2016) Le Néolithique moyen de la Corse revisité : nouvelles données, nouvelles  
12 1176 perceptions. In : Perrin T, Chambon P, Gibaja JF, Goude G(eds), *Le Chasséen, des Chasséens... Retour sur une*  
13 1177 *culture nationale et ses parallèles, Sepulcres de fossa, Cortaillod, Lagozza*. Actes du colloque international tenu  
14 1178 à Paris (France) du 18 au 20 novembre 2014, Archives d'Ecologie Préhistorique, 59-72.  
15 1179  
16 1180 Vacchi M, Marriner N, Morhange C, Spada G, Fontana A, Rovere A(2016) Multiproxy assessment of Holocene  
17 1181 relative sea-level changes in the western Mediterranean: sea-level variability and improvements in the definition  
18 1182 of the isostatic signal. *Earth Sci. Rev.* 155: 172-197.  
19 1183  
20 1184 Vacchi M, Ghilardi M, Melis RT, Spada G, Giaime M, Marriner N, Lorscheid T, Morhange C, Burjachs F, Rovere  
21 1185 A (2018) New relative sea-level insights into the isostatic history of the Western Mediterranean. *Quat. Sci. Rev.*  
22 1186 201: 396e408.  
23 1187  
24 1188 Van Geel B (1978) A palaeoecological study of Holocene peat bog sections in Germany and The Netherlands.  
25 1189 *Review of Palaeobotany and Palynology* 25: 1-120.  
26 1190  
27 1191 Van Geel B (2001) Non-pollen palynomorphs, en Smol, J.P., Birks, H.J.B., Last, W.M. (eds), Tracking  
28 1192 Environmental Change using Lake Sediments: Terrestrial, Algal, and Siliceous Indicators, 3. Kluwer, Dordrecht,  
29 1193 99–119.  
30 1194  
31 1195 Van Geel B, Mur LR, Ralska-Jasiewiczowa M (1994) Fossil akinetes of Aphanizomenon and Anabaena as  
32 1196 indicators of medieval phosphate-eutrophication of Lake Gosciadz (Central Poland). *Rev. Palaeobot. Palynol.* 83:  
33 1197 97–105.  
34 1198  
35 1199 Van Geel B, Buurman J, Brinkkemper O, Schelvis J, Aptroot A, van Reenen G, Hakbijl T (2003) Environmental  
36 1200 reconstruction of a Roman Period settlement site in Uitgeest (The Netherlands), with special reference to  
37 1201 coprophilous fungi. *J. Archaeol.Sci.* 30: 873–883.  
38 1202  
39 1203 Vella MA, Andrieu-Ponel V, Cesari J, Leandri F, Peche-Quilichini K, Reille M, Poher Y, Demory F, Delanghe D,  
40 1204 Ghilardi M, Ottaviani-Spella MD (2019) Early impact of agropastoral activities and climate on the littoral  
41 1205 landscape of Corsica since mid-Holocene. *PLoS One* 14 (12) : e0226358.  
42 1206  
43 1207 Vellutini PJ, Orsini JB, Michon G, Brisset F, CocheméJJ(1985). *Carte géologique France (1/50000), feuille*  
44 1208 *Galeria-Osani (1109)*. Orléans, BRGM.  
45 1209  
46 1210 Vellutini PJ, RossiP, Michon G, Hervé JY (1996) *Notice explicative, Carte géol. France (1/50000), feuille*  
47 1211 *Galeria-Osani (1109)*. Orléans, BRGM, 109 p.  
48 1212  
49 1213 Wanner H, Solomina O, Grosjean M, Ritz SP, Jetel M (2011) Structure and origin of Holocene cold events. *Quat.*  
50 1214 *Sci. Rev.* 30 (21–22): 3109-3123.  
51 1215  
52 1216 Yll EI, Perez-Obiol R, Pantaleon-Cano J, Roure J M (1997). Palynological evidence for climatic change and  
53 1217 human activity during the Holocene on Minorca (Balearic Islands). *Quaternary Research*, 48(3): 339-347.  
54 1218  
55 1219  
56 1220  
57 1221  
58 1222  
59 1223  
60 1224

## Figure captions

1

2

3 1225 Figure 1 : Location map of the study area. Locator map: SF: Saint Florent. Digital Elevation Model is  
 4 1226 derived from BDAlti data from IGN. Red stars indicate the location of the studied sites ;  
 5 1227 Green circle : core drilled at Crovani pond (Di Rita et al., 2022a)

7 1228 Figure 2 : Geology, topography and archaeology of the Girolata-Novalla catchment. A : Geological  
 8 1229 background and core location (geological data are derived from the 1 :50 000 scale map of  
 9 1230 Osani ; Vellutini et al., 1985 and 1996). 1: Girolata ; 2 : A Chjesaccia ; 3 : Calanchelle ; 4 :  
 10 1231 Novalla ; 5 : Girolata Fort ; 6 : modern shipwrecks (16th-18th centuries CE). B : View to the  
 11 1232 south of the Girolata Plain and Gulf (source : J.B. Mary) with coring location and main  
 12 1233 archaeological site.

15 1234 Figure 3 : Geology, topography and archaeology of the lower reaches of the Fangu catchment. A :  
 16 1235 Geological background and core location (geological data are derived from the 1 :50 000  
 17 1236 scale map of Osani ; Vellutini et al., 1985 and 1996). Yellow circle : site from the First phase  
 18 1237 (1541-1553 cal. CE) of the Genoese administration of Corsica ; 1 : Galeria tower. B : Aerial  
 19 1238 view to the south of the Fangu Estuary with coring and main archaeological site locations.

22 1239 Figure 4 : Depth/Age model for Fangu and Girolata 2 cores calculated with Clam 2.2 (Blaauw, 2010)  
 23 1240 based on 10 and 6 radiocarbon dates, respectively. The model takes into account the  $2\sigma$ -  
 24 1241 confidence range of the calibrated ages. While linear interpolation fitted well to  
 25 1242 radiocarbon data in the case of Girolata 2, the use of the smoothing spline method in the  
 26 1243 Fangu sequence provided an age-depth curve closer to the radiocarbon data.

28 1244  
 29 1245 Figure 5 :Chronostratigraphy of Girolata 1core

30 1246 Figure 6 :Chronostratigraphy of Girolata 2core

32 1247 Figure 7 :Chronostratigraphy of Fangu core

34 1248 Figure 8 : Pollen and NPP percentage diagrams for Girolata 2 core. White curves with depth bars show  
 35 1249 exaggerated curves x2; white curves, exaggeration x5; dots represent occurrences of <1%.

37 1250 Figure 9 : Pollen and NPP percentage diagrams for Fangu core. White curves with depth bars show  
 38 1251 exaggerated curves x2; white curves, exaggeration x5; dots represent occurrences of <1%.

40 1252 Figure 10 : Palaeogeographic reconstruction for the Girolata coastal plain for the last four millennia.

42 1253 Figure 11 : Diagram showing the evolution of arboreal pollen and anthropogenic indicators in Fangu,  
 43 1254 Girolata 2, Crovani and Saint Florent cores for the last six millennia. Chronology of the cultural periods  
 44 1255 for Prehistory and Protohistory is derived from Tramoni and D'Anna (2016). Categories: OVJC (*Olea*,  
 45 1256 *Vitis*, *Juglans*, *Castanea*), Ruderals (*Rumex*, Brassicaceae, *Polygonum*, *Plantago*, *Urtica*), Coprophilous  
 46 1257 fungi (*Sordaria*-t, *Sporormiella*, *Cercophora*-t, *Podospora*-t, *Delitschia*). Colour frames indicate the four  
 47 1258 main phases of forest decline and grey frames indicate episodes of human impact without clear forest  
 48 1259 decline. Bond events (Bond et al., 1997) and RCC events (Mayewski et al., 2004) are reported on the  
 49 1260 graph.

52 1261 Figure 12 : Arboreal pollen (AP) evolution from the Iron Age onwards according to chronocultural  
 53 1262 periods for the sites of Saint-Florent (Nebbiu) ; Crovani (Balagne) ; Fangu and Girolata (Filosorma). The  
 54 1263 five major forest declines identified with palynology are highlighted with dashed grey bands; Event 2  
 55 1264 alone is not documented in any known literary source. In the locator map : SF : Saint-Florent ; Cr. :  
 56 1265 Crovani ; Fa. : Fangu ; Gi. : Girolata; Sa. : Sagone.

59 1266  
 60

1  
2  
3 1267 Table 1 : Borehole information.  
4

5 1268 Table 2 : Radiocarbon dating results. Samples indicated by an \* were rejected by the depth/age model  
6 1269 calculation.  
7

8 1270  
9

### 10 1271 **Authors' contributions**

11 1272  
12 1273 All authors have materially participated in the research project and article preparation, as follows.  
13 1274 Conceptualization: MG, JR, FDR. Sediment collection: MG and JBM and LM. Methodology: MG, JR, FDR,  
14 1275 DD. Formal analyses: MG, JR, JBM, CD, DD, and SR. Data collection: MG, JR, JBM, CD, DD. Results  
15 1276 interpretation: MG, JR, JBM, FDR. Writing original draft: MG, JR. Contribution in interpreting results  
16 1277 and writing the paper: MG, JR, FDR. Funding acquisition: MG, JBM.  
17 1278

18 1278

19 1279

### 20 1280 **Declaration of competing interest**

21 1281  
22 1282 The authors declare that they have no known competing financial interests or personal relationships  
23 1283 that could have appeared to influence the work reported in this paper.  
24  
25  
26  
27  
28  
29  
30  
31  
32  
33  
34  
35  
36  
37  
38  
39  
40  
41  
42  
43  
44  
45  
46  
47  
48  
49  
50  
51  
52  
53  
54  
55  
56  
57  
58  
59  
60

1  
2  
3  
4  
5  
6  
7  
8  
9  
10  
11  
12  
13  
14  
15  
16  
17  
18  
19  
20  
21  
22  
23  
24  
25  
26  
27  
28  
29  
30  
31  
32  
33  
34  
35  
36  
37  
38  
39  
40  
41  
42  
43  
44  
45  
46

Site	Core id	Elevation amsl (in m, error : ± 0.1 m)	Length (in m)	X (WGS 84)	Y (WGS 84)	Easting (RGF/Lambert 93)	Northing (RGF/Lambert 93)
Girolata	Girolata 1	+ 0,88	3.15	8°36'51.95"E	42°21'2.67"N	1162962,28	6155430,50
	Girolata 2	+ 0,85	4.20	8°36'44.17"E	42°21'0.03"N	1162791,59	6155337,24
Fangu	Fangu	+ 0,70	4.20	8°39'34.07"E	42°25'7.83"N	1166123,87	6163257,70

Table 1 : Boreholes location. Elevation is derived from Litto3D survey (SHOM-Collectivité de Corse-DREAL, 2020)

Core id	Depth (in m)	Elevation amsl (in m)	Material	BP	Error ±	Cal ages	Lab. code
Girolata 1	1,66	-0,78	<i>Posidonia oceanica</i>	3280	30	1317-917 BCE	Poz-129246
	2,96	-2,08	<i>Posidonia oceanica</i>	3375	35	1424-1047 BCE	Poz-128585
Girolata 2	0,68	+0,17	Organic sediment	740	30	1226-1297 CE	Poz-129251
	0,96	-0,11	Organic sediment	1770	30	222-375 CE	Poz-129248
	1,33	-0,48	Charcoal	2455	30	754-415 BCE	Poz-129249
	2,66	-1,81	<i>Posidonia oceanica</i>	3125	30	1119-769 BCE	Poz-128586
	2,98	-2,13	Organic sediment	3115	30	1447-1286 BCE	Poz-129250
	4,1	-3,25	Charcoal	3495	35	1921-1696 BCE	Poz-128587
Fangu	0,48	+0,22	Charcoal	805	30	1179-1277 CE	Poz-141492
	0,6	+0,1	Charcoal	1215	30	689-889 CE	Poz-141286
	0,79	-0,09	Plant remains	130	30	1673-1942 CE*	Poz-145856
	1,74	-1,04	Charcoal	3550	30	2013-1772 BCE	Poz-145857
	1,87	-1,17	Charcoal	3655	35	2140-1929 BCE	Poz-141287
	2,35	-1,65	Charcoal	4050	35	2925-2693 BCE	Poz-144578
	2,71	-2,01	Charcoal	4755	35	3640-3376 BCE*	Poz-145858
	3,05	-2,35	Plant remains	4375	35	3092-2907 BCE	Poz-144494
	3,75	-3,05	Wood ( <i>Pinus nigra/sylvestris</i> )	5000	40	3945-3653 BCE	Poz-145859
4,12	-3,42	Plant remains	4250	40	2672-2470 BCE*	Poz-144493	

Table 2 : Radiocarbon dating results

1  
2  
3  
4  
5  
6  
7  
8  
9  
10  
11  
12  
13  
14  
15  
16  
17  
18  
19  
20  
21  
22  
23  
24  
25  
26  
27  
28  
29  
30  
31  
32  
33  
34  
35  
36  
37  
38  
39  
40  
41  
42  
43  
44  
45  
46  
47  
48  
49  
50  
51  
52  
53  
54  
55  
56  
57  
58  
59  
60

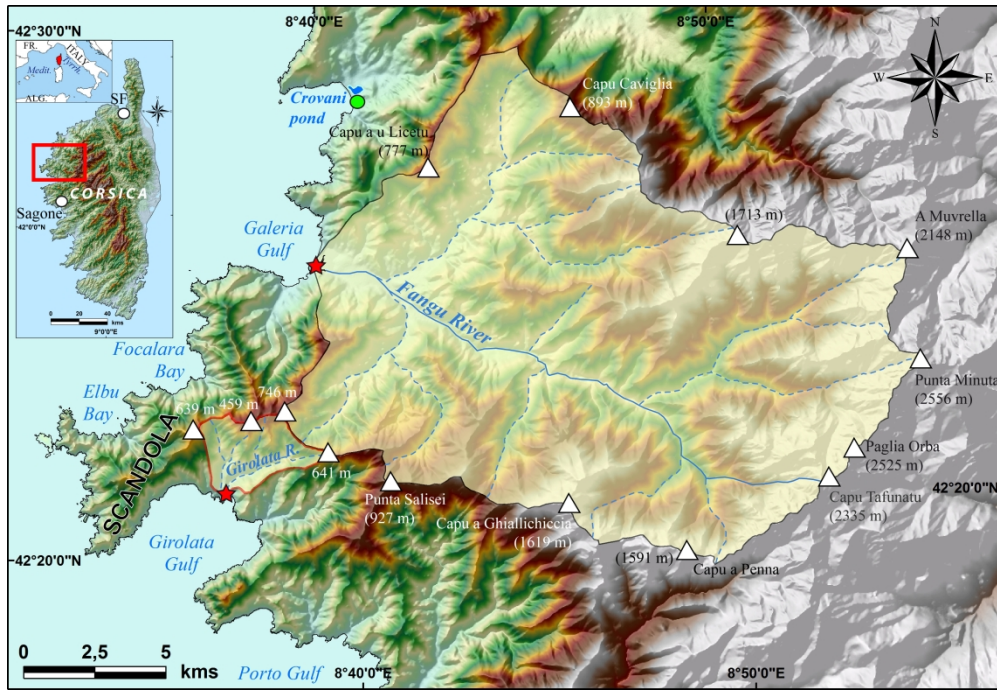


Figure 1: Location map of the study area. Locator map: SF: Saint Florent. Digital Elevation Model is derived from BDAlti data from IGN. Red stars indicate the location of the studied sites ; Green circle : core drilled at Crovani pond (Di Rita et al., 2022a)

293x200mm (300 x 300 DPI)

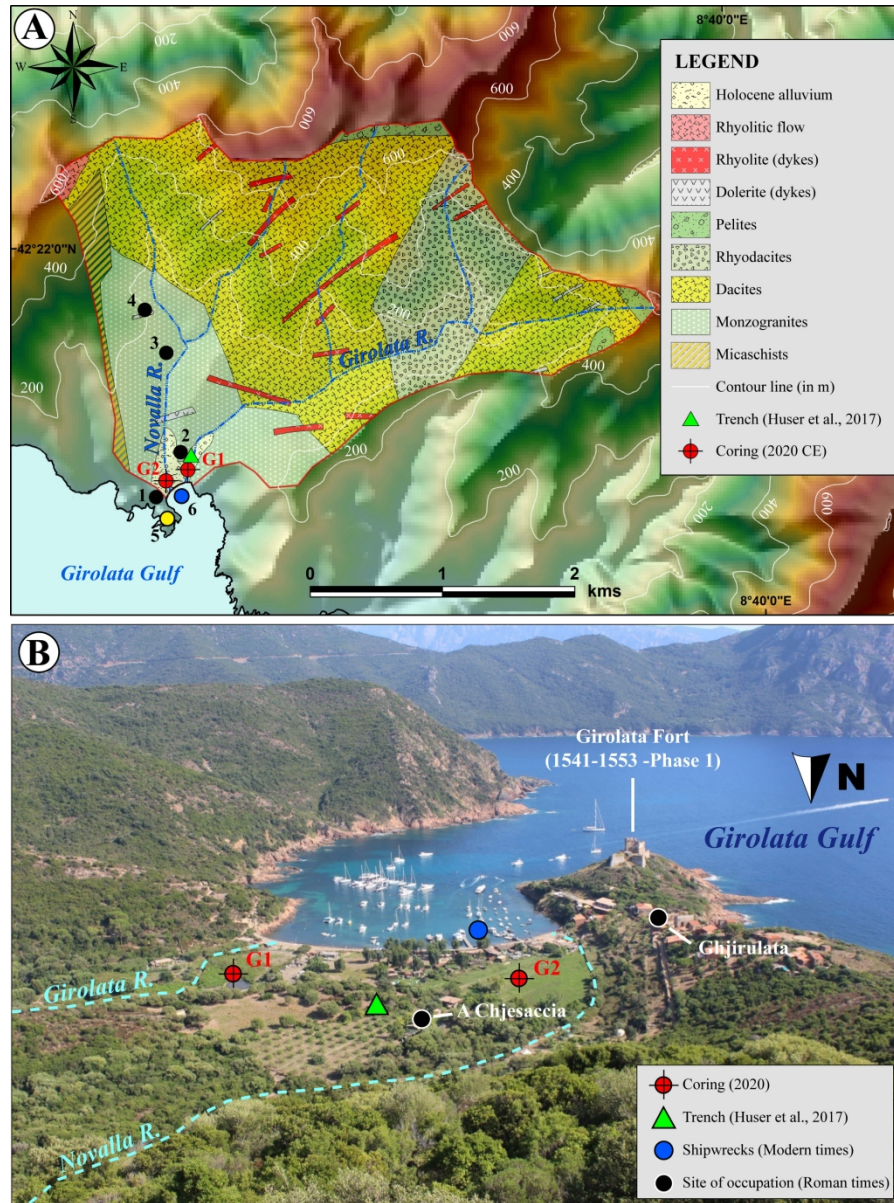


Figure 2 : Geology, topography and archaeology of the Girolata-Novalla catchment. A : Geological background and core location (geological data are derived from the 1 :50 000 scale map of Osani ; Vellutini et al., 1985 and 1996). 1 : Girolata ; 2 : A Chjesaccia ; 3 : Calanchelle ; 4 : Novalla ; 5 : Girolata Fort ; 6 : modern shipwrecks (16th-18th c. CE). B : View to the south of the Girolata Plain and Gulf (source : J.B. Mary) with coring location and main archaeological site.

204x276mm (300 x 300 DPI)



1  
2  
3  
4  
5  
6  
7  
8  
9  
10  
11  
12  
13  
14  
15  
16  
17  
18  
19  
20  
21  
22  
23  
24  
25  
26  
27  
28  
29  
30  
31  
32  
33  
34  
35  
36  
37  
38  
39  
40  
41  
42  
43  
44  
45  
46  
47  
48  
49  
50  
51  
52  
53  
54  
55  
56  
57  
58  
59  
60

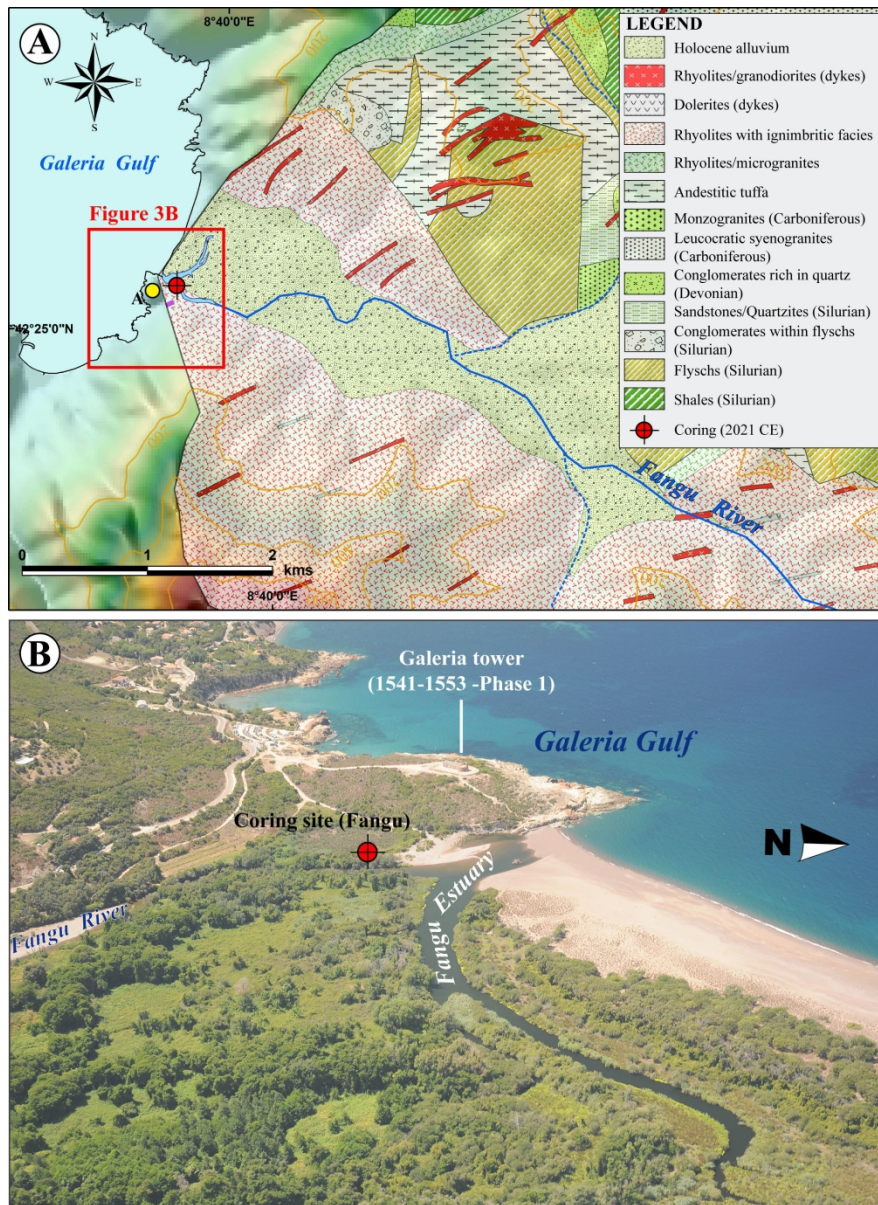


Figure 3 : Geology, topography and archaeology of the lower reaches of the Fangu catchment. A : Geological background and core location (geological data are derived from the 1 :50 000 scale map of Osani ; Vellutini et al., 1985 and 1996). Yellow circle : site from the First phase (1541-1553 cal. CE) of the Genoese administration of Corsica ; 1 : Galeria tower. B : Aerial view to the south of the Fangu Estuary with coring and main archaeological site locations.

205x279mm (300 x 300 DPI)

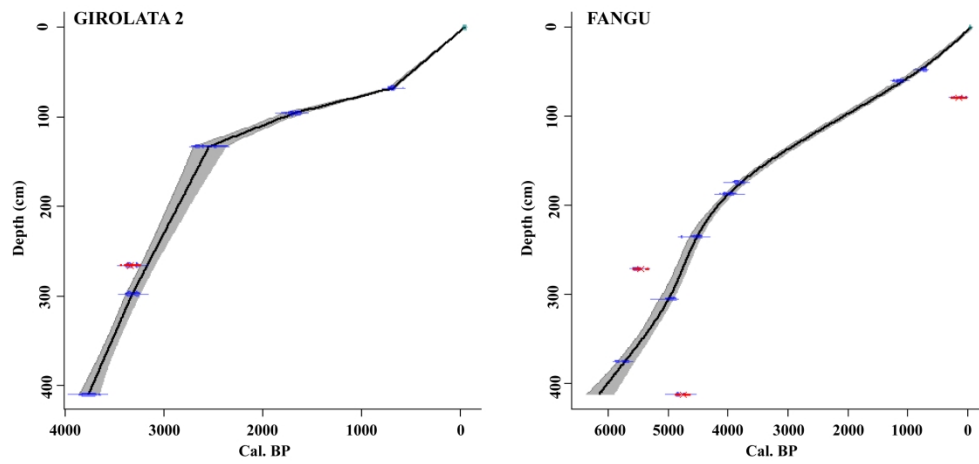


Figure 4: Depth/Age model for Fangu and Girolata 2 cores calculated with Clam 2.2 (Blaauw, 2010) based on 10 and 6 radiocarbon dates, respectively. The model takes into account the  $2\sigma$ -confidence range of the calibrated ages. While linear interpolation fitted well to radiocarbon data in the case of Girolata 2, the use of the smoothing spline method in the Fangu sequence data provided an age-depth curve closer to the radiocarbon data.

267x127mm (300 x 300 DPI)

1  
2  
3  
4  
5  
6  
7  
8  
9  
10  
11  
12  
13  
14  
15  
16  
17  
18  
19  
20  
21  
22  
23  
24  
25  
26  
27  
28  
29  
30  
31  
32  
33  
34  
35  
36  
37  
38  
39  
40  
41  
42  
43  
44  
45  
46  
47  
48  
49  
50  
51  
52  
53  
54  
55  
56  
57  
58  
59  
60

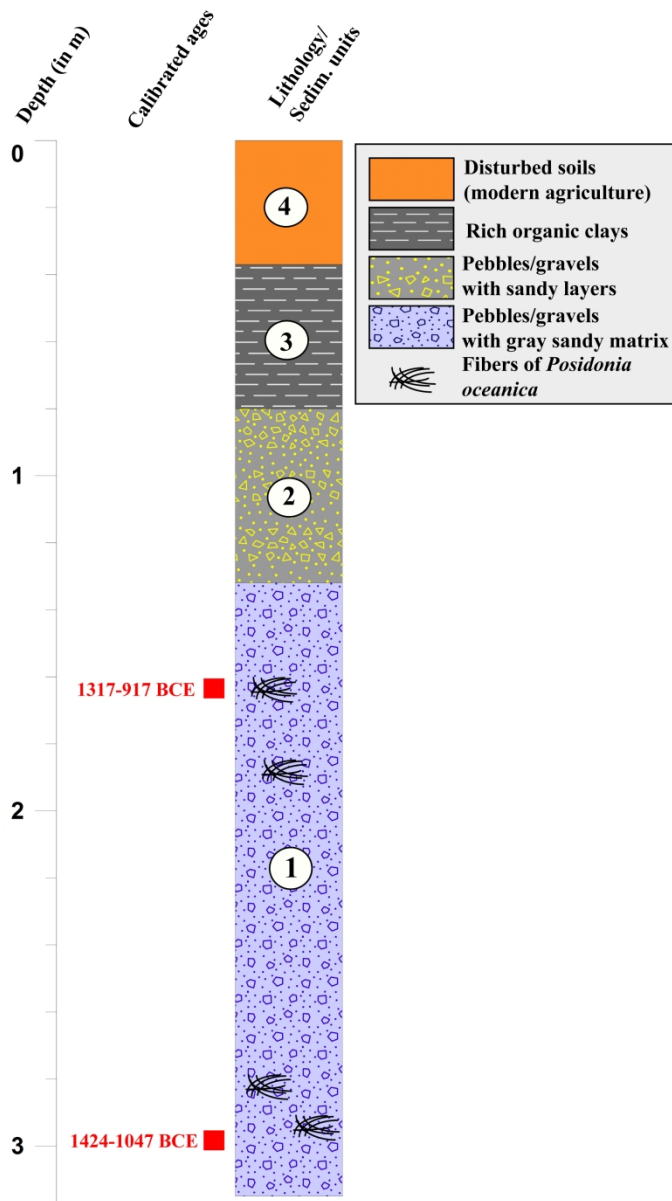


Figure 5 : Chronostratigraphy of Girolata 1 core

163x284mm (300 x 300 DPI)

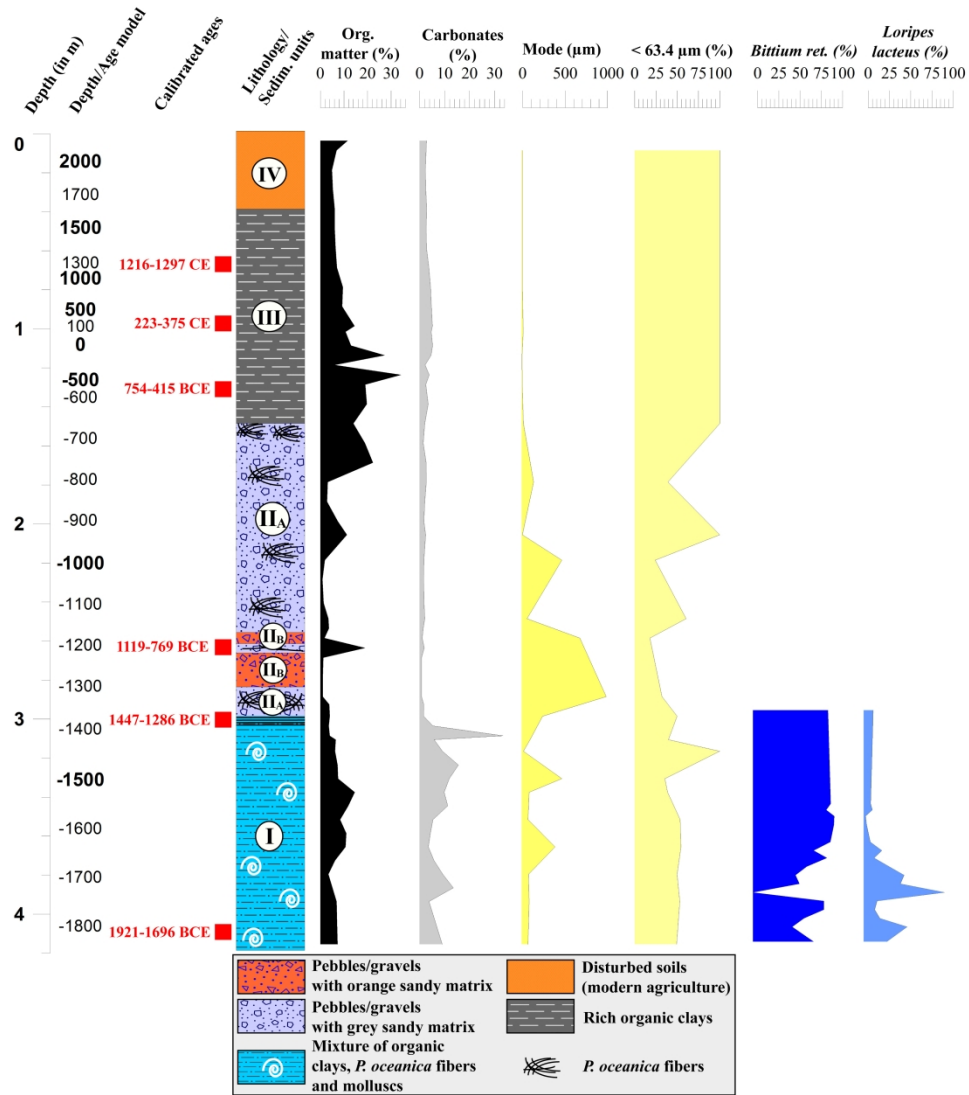


Figure 6 : Chronostratigraphy of Girolata 2core

298x325mm (300 x 300 DPI)

1  
2  
3  
4  
5  
6  
7  
8  
9  
10  
11  
12  
13  
14  
15  
16  
17  
18  
19  
20  
21  
22  
23  
24  
25  
26  
27  
28  
29  
30  
31  
32  
33  
34  
35  
36  
37  
38  
39  
40  
41  
42  
43  
44  
45  
46  
47  
48  
49  
50  
51  
52  
53  
54  
55  
56  
57  
58  
59  
60

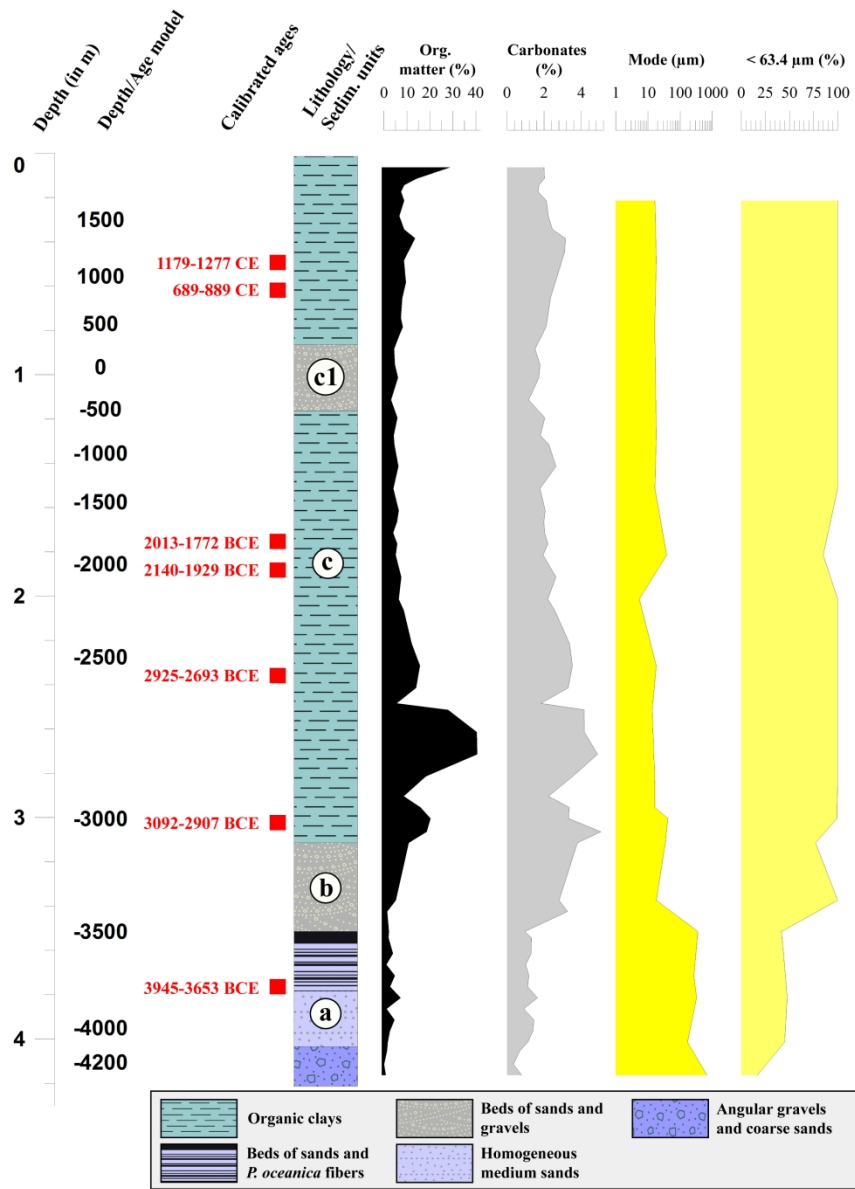


Figure 7 : Chronostratigraphy of Fangu core

225x315mm (300 x 300 DPI)

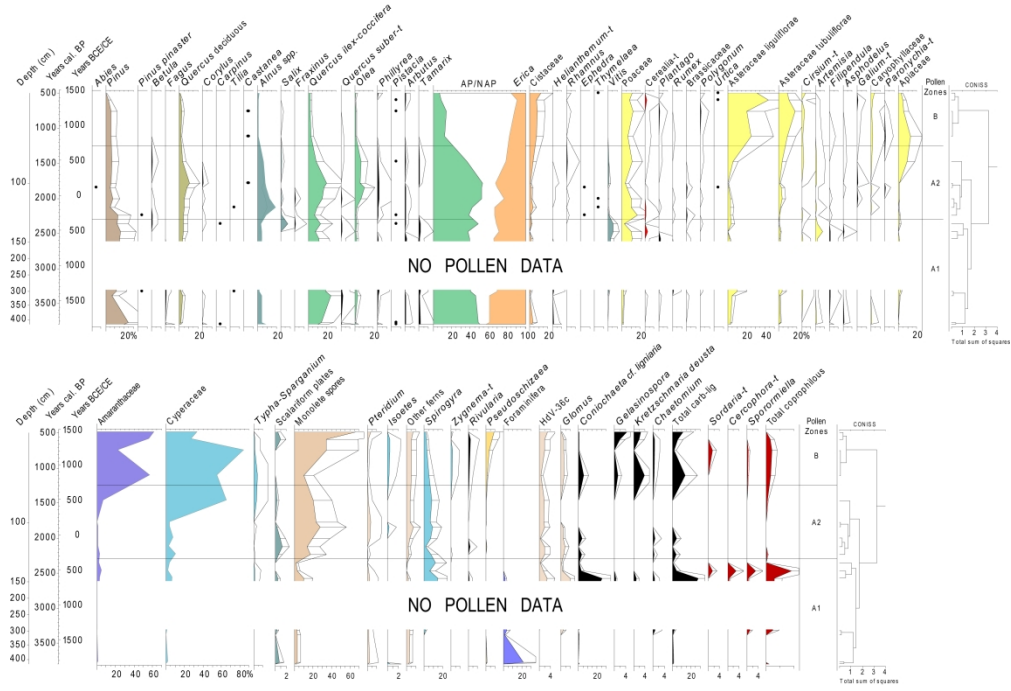


Figure 8 : Pollen and NPP percentage diagrams for Girolata 2 core. White curves with depth bars show exaggerated curves x2; white curves, exaggeration x5; dots represent occurrences of <1%.

292x199mm (300 x 300 DPI)

1  
2  
3  
4  
5  
6  
7  
8  
9  
10  
11  
12  
13  
14  
15  
16  
17  
18  
19  
20  
21  
22  
23  
24  
25  
26  
27  
28  
29  
30  
31  
32  
33  
34  
35  
36  
37  
38  
39  
40  
41  
42  
43  
44  
45  
46  
47  
48  
49  
50  
51  
52  
53  
54  
55  
56  
57  
58  
59  
60

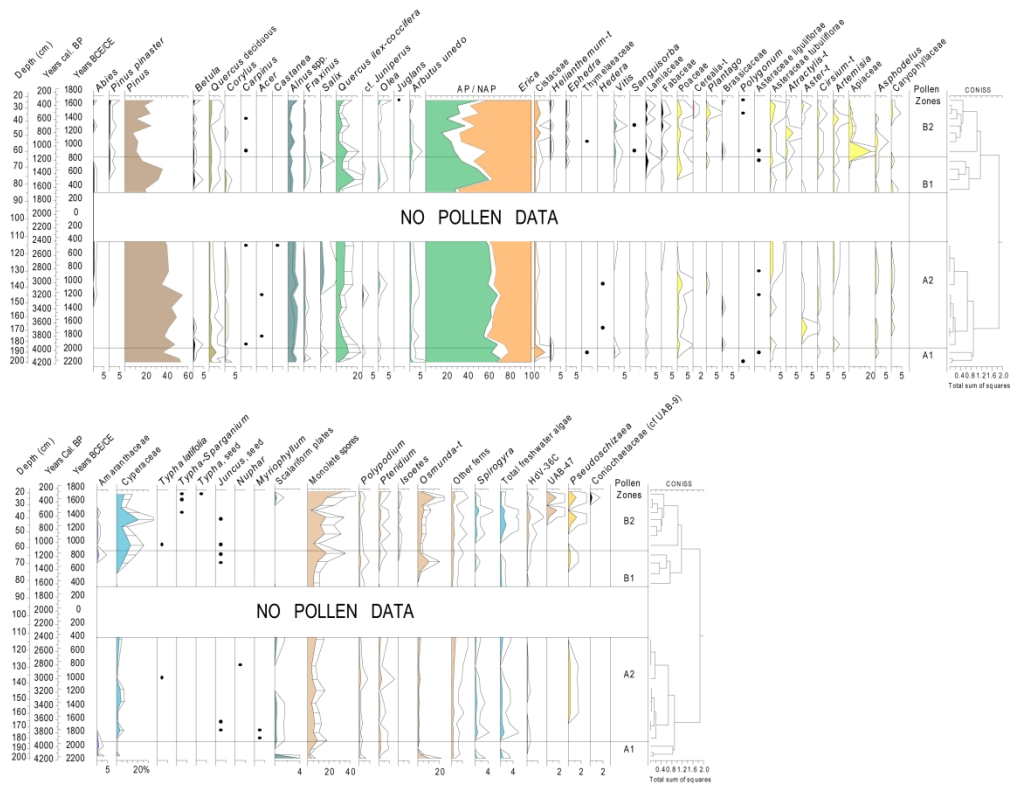


Figure 9 : Pollen and NPP percentage diagrams for Fangu core. White curves with depth bars show exaggerated curves x2; white curves, exaggeration x5; dots represent occurrences of <1%.

287x222mm (300 x 300 DPI)

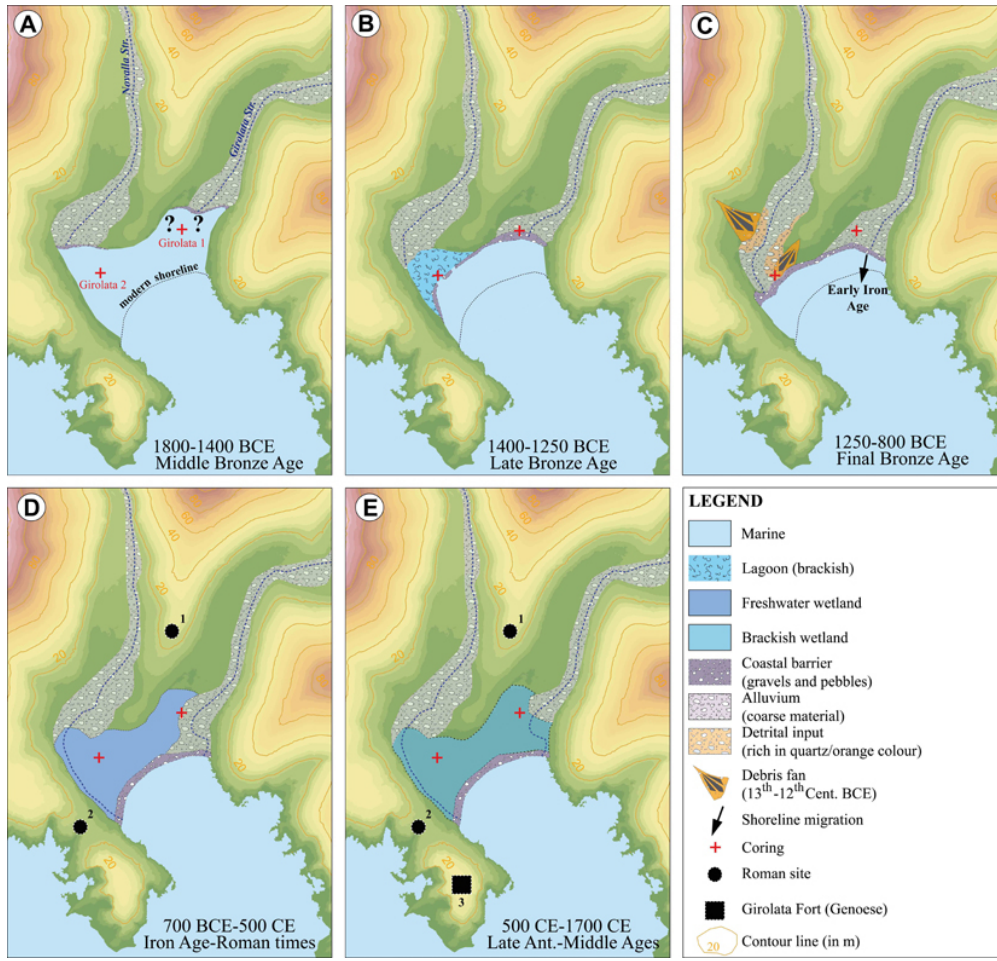


Figure 10 : Palaeogeographic reconstruction for the Girolata coastal plain for the last four millennia.

600x571mm (35 x 35 DPI)



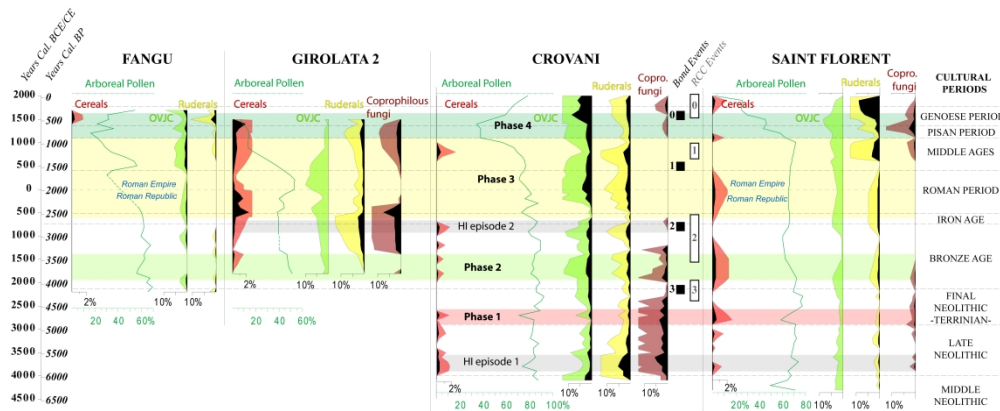


Figure 11 : Diagram showing the evolution of arboreal pollen and anthropogenic indicators in Fangu, Girolata 2, Crovani and Saint Florent cores for the last six millennia. Chronology of the cultural periods for Prehistory and Protohistory is derived from Tramoni and D'Anna (2016). Categories: OVJC (Olea, Vitis, Juglans, Castanea), Ruderals (Rumex, Brassicaceae, Polygonum, Plantago, Urtica), Coprophilous fungi (Sordaria-t, Sporormiella, Cercophora-t, Podospora-t, Delitschia). Colour frames indicate the four main phases of forest decline and grey frames indicate episodes of human impact without clear forest decline. Bond events (Bond et al., 1997) and RCC events (Mayewski et al., 2004) are reported on the graph.

386x156mm (300 x 300 DPI)

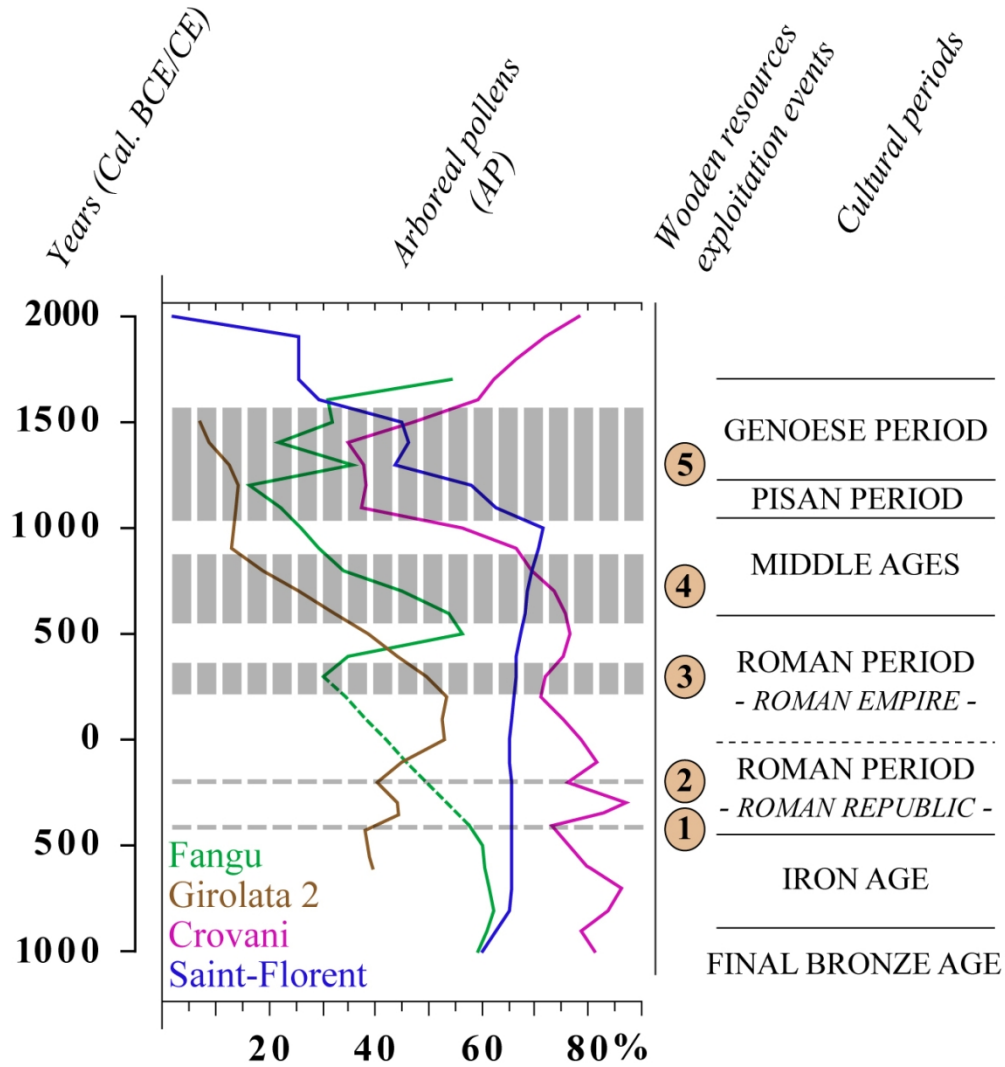


Figure 12 : Arboreal pollen (AP) evolution from the Iron Age onwards according to chronocultural periods for the sites of Saint-Florent (Nebbiu) ; Crovani (Balagne) ; Fangu and Girolata (Filosorma). The five major forest declines identified with palynology are highlighted with dashed grey bands; Event 2 alone is not documented in any known literary source. In the locator map : SF : Saint-Florent ; Cr. : Crovani ; Fa. : Fangu ; Gi. : Girolata ; Sa. : Sagone.

112x120mm (300 x 300 DPI)